

Temporal integration of narrative information in a hippocampal amnesic patient

Xiaoye Zuo^{a,*}, Christopher J. Honey^a, Morgan D. Barense^{b,c}, Davide Crombie^d, Kenneth A. Norman^{e,f}, Uri Hasson^{e,f}, Janice Chen^a

^a Department of Psychological and Brain Sciences, Johns Hopkins University, Baltimore, MD, 21218, USA

^b Department of Psychology, University of Toronto, Toronto, Ontario, M5S 3G3, Canada

^c Rotman Research Institute, Baycrest Hospital, Toronto, Ontario, M5S 3G3, Canada

^d Department of Biology II - Neurobiology, Ludwig Maximilian University of Munich, Großhaderner Str. 2, 82152, Planegg, Germany

^e Princeton Neuroscience Institute, Princeton University, Princeton, NJ, 08544, USA

^f Department of Psychology, Princeton University, Princeton, NJ, 08544, USA

ABSTRACT

Default network regions appear to integrate information over time windows of 30 s or more during narrative listening. Does this long-timescale capability require the hippocampus? Amnesic behavior suggests that regions other than the hippocampus can independently support some online processing when input is continuous and semantically rich: amnesics can participate in conversations and tell stories spanning minutes, and when tested immediately on recently heard prose they are able to retain some information. We hypothesized that default network regions can integrate the semantically coherent information of a narrative across long time windows, even in the absence of an intact hippocampus. To test this prediction, we measured BOLD activity in the brain of a hippocampal amnesic patient (D.A.) and healthy control participants while they listened to a 7 min narrative. The narrative was played either in its intact form, or as a paragraph-scrambled version, which has been previously shown to interfere with the long-range temporal dependencies in default network activity. In the intact story condition, D.A.'s moment-by-moment BOLD activity spatial patterns were similar to those of controls in low-level auditory cortex as well as in some high-level default network regions (including lateral and medial posterior parietal cortex). Moreover, as in controls, D.A.'s response patterns in medial and lateral posterior parietal cortex were disrupted when paragraphs of the story were presented in a shuffled order, suggesting that activity in these areas did depend on information from 30 s or more in the past. Together, these results suggest that some default network cortical areas can integrate information across long timescales, even when the hippocampus is severely damaged.

1. Introduction

People with hippocampal damage are profoundly impaired in recalling information after a distraction (Milner, 1966), or “as soon as their attention shifts to a new topic” (Milner, 2005). At the same time, these amnesic individuals are able to engage in conversation, retain near-normal immediate recall for prose passages (Baddeley and Wilson, 2002), and can sometimes tell globally coherent stories (Keven et al., 2018; Kurczek and Duff, 2011; Rosenbaum et al., 2009). How is this possible? The traditional explanation is that amnesics rely on working memory processes and active rehearsal (e.g., phonological loop) to compensate for their impairments in episodic recollection. However, a new view argues that classic working memory accounts, while good descriptors for tasks requiring goal-directed control of prior information, do not apply in cases of continuous natural input such as stories and conversation (Hasson et al., 2015). Instead, default network areas are proposed to carry slowly-changing information during such

semantically-rich naturalistic episodes, across timescales of around 30 s. Unlike in working memory tasks, retention of information across time during a story or conversation is not via effortful active maintenance, but rather occurs via continuous integration of new input with prior information in the service of comprehension. Thus, in the absence of major topic changes or surprises that create a distraction, amnesic individuals might be able to rely on default network cortical regions for retention of information across “long timescales” of around 30 s.

It is an open question whether the long-timescale capability of default network regions critically depends on interactions with the hippocampus, or whether they have some intrinsic memory (Hasson et al., 2015; Chen et al., 2016). The hippocampus is clearly needed for tasks that involve retrieving isolated memoranda after 30 s without active rehearsal. In healthy people, default network areas are functionally coupled to the hippocampus and seem to work together to accumulate, maintain, and integrate information across events (van Kesteren et al., 2010; Ranganath and Ritchey, 2012; Chen et al., 2016). In cases of

* Corresponding author.

E-mail addresses: zoeyzuo@jhu.edu, zoey.zuo@mail.utoronto.ca (X. Zuo).

<https://doi.org/10.1016/j.neuroimage.2020.116658>

Received 21 July 2019; Received in revised form 6 February 2020; Accepted 13 February 2020

Available online 19 February 2020

1053-8119/© 2020 The Authors. Published by Elsevier Inc. This is an open access article under the CC BY-NC-ND license (<http://creativecommons.org/licenses/by-nc-nd/4.0/>).

hippocampal and medial temporal lobe (MTL) damage, functional connectivity between the hippocampus/MTL and default network areas is altered (Frings et al., 2009; Hayes et al., 2012; McCormick et al., 2013). Thus, it is plausible that the default network retains information across long timescales due purely to retrieval and reactivation processes instigated by the hippocampus. On the other hand, slower dynamics in higher-order areas have been modeled as arising from local recurrent connections and cortico-cortical interactions (Chaudhuri et al., 2015), not from hippocampus; these slow dynamics are hypothesized to enable intrinsic memory in the default network (Honey et al., 2012; Stephens et al., 2013). MTL damage does not impact connectivity among default network nodes during resting state (Hayes et al., 2012). And, as mentioned above, hippocampal amnesics can engage in conversation and tell somewhat coherent stories, suggesting that these abilities are at least partially preserved somewhere else in the brain.

In this study, we investigated whether default network areas can integrate information over tens of seconds even without an intact hippocampus by recording the brain activity of a hippocampal amnesic patient as he listened to an auditory story. Narratives that unfold over minutes are suitable to test such a question, as they require the integration of incoming information with relevant information presented many sentences ago. For example, the meaning of an incoming sentence, e.g., “X entered the bank”, will be different as a function of information presented earlier in the story, e.g., X is a robber versus X is an investor. In previous studies, we demonstrated that (in neurotypical subjects) default network responses for a given paragraph of a story were changed if the preceding paragraph was changed by scrambling the order of paragraphs (Lerner et al., 2011); since each paragraph was on average 30 s long, the results indicate that default network activity patterns depend on information accumulated across at least the last 30 s of the story, i.e., long-timescale integration (Supplementary Fig. 1). (Windows longer than 30 s have not been tested.) This scrambling technique was used with different window sizes to map a hierarchy of timescales across the cortex: default network areas had the longest timescales (around 30 s), intermediate areas along the superior temporal gyrus had sentence-length (hundreds of milliseconds) timescales, and early sensory areas were found to operate at timescales shorter than a word (tens of milliseconds) (Hasson et al., 2008; Honey et al., 2012; Lerner et al., 2011).

We hypothesized that default network areas would exhibit long-timescale integration properties even in the absence of the hippocampus. This hypothesis makes two key predictions: 1) when amnesic patients listen to an intact story, their default network moment-by-moment activity patterns should match those of controls above chance; and 2) amnesic response patterns in the default network should be disrupted when paragraphs of the story are presented in a shuffled order. We tested these predictions with two primary analyses.

Analysis 1: *Intact Story Match*. As described above, in neurotypical subjects the activity patterns of default network areas for each paragraph in an intact story depend on the content presented in prior paragraphs. Thus, if amnesic default network responses do not match those of controls above chance during intact story listening, it suggests that the default network inherited its long-timescale context sensitivity solely from the hippocampus, i.e., without hippocampus, long-timescale context sensitivity in the amnesic’s default network is so disrupted as to be undetectable. Conversely, if amnesic default network responses do match those of controls above chance during intact story listening, two (non-exclusive) factors remain to explain the similarity: non-hippocampally-dependent (intrinsic) long-timescale information, and intrinsic short-timescale information. Intrinsic short-timescale information is very likely to exist in the default network, based on prior studies showing above-chance similarity between intact and paragraph-scrambled stories (Lerner et al., 2011). Thus, the next analysis is designed to test for intrinsic long timescales in the presence of intrinsic short timescale information in the default network.

Analysis 2: *Unscrambling*. In neurotypical subjects, default network activity patterns for a given paragraph are changed if the preceding

paragraph is changed, e.g., by temporally re-ordering the paragraphs (Lerner et al., 2011). The temporal re-ordering of paragraphs removes the contribution of long-timescale information in default network responses. Specifically, when activity patterns are compared between a person listening to the intact story and another person listening to the paragraph-scrambled story, matching paragraph-by-paragraph (intact-vs-scrambled), the similarity is lower in the default network than when comparing between two people both listening to the intact story (intact-vs-intact). The similarity between intact-vs-intact is driven by long-timescale information and short-timescale information; the similarity between intact-vs-scrambled is driven by short-timescale information only. A significant drop is predicted from intact-vs-intact to intact-vs-scrambled in the default network.

In an amnesic patient, hippocampal contributions to default network long timescales are absent or greatly reduced. Thus, the similarity between intact (control)-vs-intact (patient) in the default network can be driven by intrinsic long-timescale information and intrinsic short-timescale information; the similarity between intact (control)-vs-scrambled (patient) can be driven by short-timescale information only. If intrinsic long-timescale information does not exist in the default network, then there is nothing to be removed by paragraph scrambling, and thus intact-vs-scrambled similarity should not be significantly lower than intact-vs-intact similarity. Conversely, if intact-vs-scrambled similarity is significantly lower than intact-vs-intact similarity, this would provide critical evidence that intrinsic long-timescale information does exist in the default network.

Note that the above analyses test whether the default network has any detectable intrinsic (non-hippocampally-dependent) long timescale context sensitivity; however, our results should not be taken to answer the question of whether default network long-timescale sensitivity is completely independent of the hippocampus. Our current data do not allow us to confirm or deny this claim. We think it is likely that default network long timescales do have a hippocampally-dependent component, as studied in prior work (Chen et al., 2016).

We additionally examined response reliability of the scrambled-paragraphs stimulus alone (*Scramble Reliability*), as reduced reliability of scrambled-paragraphs relative to intact story provides complementary evidence of a region’s long-timescale integration properties (Lerner et al., 2011). As a control test, we predicted that moment-by-moment activity patterns in early auditory areas, which integrate information over short timescales, would be similar between amnesic and neurotypical subjects regardless of paragraph scrambling.

To test these predictions, we used functional magnetic resonance imaging (fMRI) to record brain responses in neurotypical control subjects and in a bilateral hippocampal amnesic patient as they listened to a 7 min auditory narrative, as well as to a version of the same stimulus temporally scrambled at the paragraph level. We observed that in some default network regions, including lateral posterior parietal cortex (PPC), posterior medial cortex (PMC), and medial prefrontal cortex (mPFC), there were significantly similar brain activity patterns between the amnesic and controls across the duration of the intact story. This similarity was observed in spite of the fact that the patient was more than 30 years older than the control subjects—i.e., the 63-year-old amnesic’s brain activity in default network regions substantially resembled that of 18–31-year-old university undergraduate students as they listened to the same real-life story. Furthermore, in both the patient and in the neurotypical control subjects, activity patterns in default network areas for a given paragraph were changed if the preceding paragraph was changed (by scrambling the order of paragraphs), supporting the notion that these brain areas carried information across 30 s or more, even without an intact hippocampus. In contrast, early auditory areas were similar between amnesic and neurotypical subjects regardless of scrambling. This case study provides novel evidence that the purported ability of default network cortical areas to integrate information across long timescales does not depend solely on interactions with the hippocampus.

2. Methods

2.1. Participants

An amnesic patient “D.A.” (age: 63 at the time of first fMRI scan session) participated in both behavioral and fMRI tasks. D.A.’s anatomical and behavioral assessments were first reported in Rosenbaum et al. (2008). D.A. became amnesic after contracting herpes encephalitis in 1993. He suffered bilateral MTL damage encompassing the entire right MTL and hippocampus, severe reductions to left MTL cortical areas, and less than 1/3 of the left hippocampus remaining; volume loss was also observed over right-hemisphere posterior temporal, ventral frontal, occipital, and anterior cingulate regions, while left-hemisphere volume loss was limited to the MTL. Small lesions were present in right posterior thalamus and left middle temporal gyrus. See Rosenbaum et al. (2008) for D.A.’s earlier anatomical images, and Fig. 1A for new brain images collected for this study in 2015. Behaviorally, he experienced extensive anterograde and graded retrograde amnesia, including memory loss of

the period just prior to the onset of amnesia and a postmorbid period, with memories from the most remote time periods spared. His scores on standard neuropsychological tests (Wechsler Memory Scale; Wechsler, 1987) are reported in Rosenbaum et al. (2008) and indicate that he has high IQ, preserved short-term memory, and severely impaired delayed memory (< 1st percentile). D.A. is a native English speaker with normal hearing and provided written informed consent in accordance with protocols that were approved by the University of Toronto and Baycrest Hospital Research Ethics Boards.

Age-matched control participants (N = 12, age range: 57–66), as well as a group of younger control participants (N = 9, age range: 18–24; see Table 1 for detailed demographic information), were recruited for behavioral tasks.

Control data for fMRI tasks came from a previous experiment, Simony et al. (2016). Thirty-six healthy participants (25 females, ages: 18–33) contributed to the Intact Story condition, and eighteen participants (12 females, ages: 18–31) contributed to the Scrambled Paragraphs condition. All subjects were native English speakers with normal hearing and

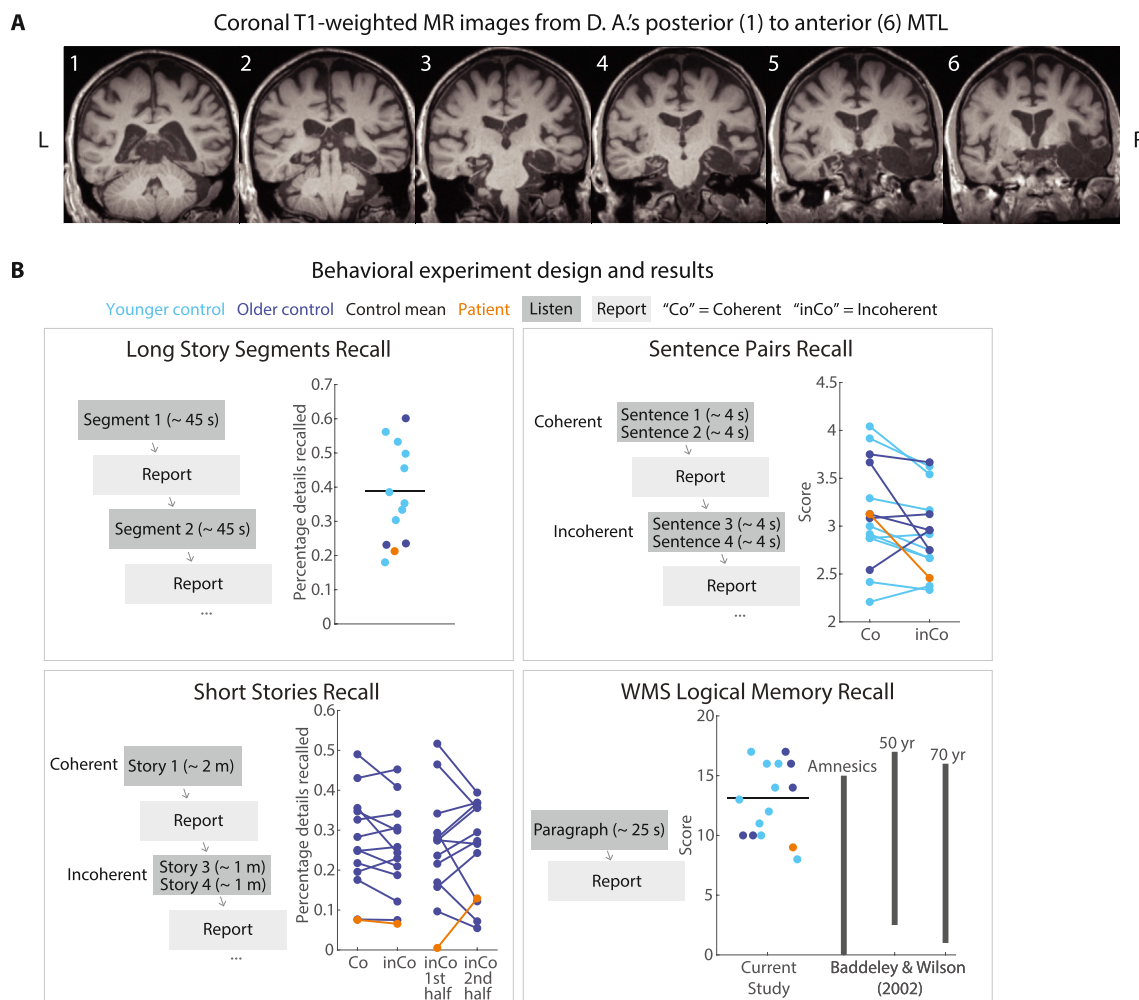


Fig. 1. Patient anatomy and behavioral performance on verbal recall tests. **A)** Coronal T1-weighted MR images from D.A.’s posterior to anterior MTL. D.A. has bilateral MTL damage that is more pronounced in the right hemisphere. The right perirhinal, entorhinal, and parahippocampal cortices, and the anterior temporal lobe, are severely damaged. Over 90% of the right hippocampus is damaged. Left perirhinal, entorhinal, and parahippocampal cortices are also severely damaged. **B)** Behavioral task design. Participants listened to four different types of auditory stimuli and verbally reported what they remembered from the stimuli immediately following presentation. In the Long Story Segments session, participants listened to segments (approximately 45 s each) from two stories, presented sequentially. Each of the 13 segments (8 from Story 1, 5 from Story 2) was followed by immediate verbal recall. In the Sentence Pairs session, participants listened to 12 coherent (Co) sentence pairs pseudo-randomly interleaved with 12 incoherent (inCo) sentence pairs, each pair lasting for approximately 4 s. Immediately following each sentence pair, participants were instructed to report the sentences verbatim. In the Short Stories session, participants listened to 4 coherent (Co) stories interleaved with 4 incoherent (inCo) short stories, each lasting approximately 2 min. The incoherent stories were created by concatenating two different stories. D.A. listened to 3 coherent and 3 incoherent short stories. In the WMS-IV Logical Memory experiment, participants listened to the “Anna Thompson” narrative (25 s) and reported back the story verbatim.

Table 1
Behavioral experiment control participants.

Session	Older adults	Younger adults	Overall
Long Story Segments	n = 3 (M age = 63.7; range = 63–64)	n = 9 (M age = 19.2; range = 18–24)	n = 12 7 females, 5 males
Sentence Pairs	n = 5 (M age = 62.6; range = 67–65)	n = 9 (M age = 19.2; range = 18–24)	n = 14 9 females, 5 males
Short Stories	n = 12 (M age = 62.8; range = 57–66)	N. A.	n = 12 8 females, 4 males
WMS	n = 5 (M age = 62.6; range = 67–65)	n = 9 (M age = 19.2; range = 18–24)	n = 14 9 females, 5 males

provided written informed consent. See [Simony et al. \(2016\)](#) for more details.

2.2. Behavioral tasks: immediate verbal recall

Task design. D.A. participated in four immediate verbal recall tasks: Long Story Segments, Sentence Pairs, Short Stories, and the Wechsler Memory Scale-IV Logical Memory Test (WMS; [Wechsler, 1987](#)). Age-matched controls and younger controls participated in the same four tasks ([Fig. 1B](#)). For D.A., all audio presentation was controlled by the experimenter and recall was verbally elicited by the experimenter, while control participants used a keyboard to self-initiate listening and recall for each trial.

Long Story Segments: Two “long stories” were used, 5 and 8 min long, each split into approximately 1 min segments. The segments were presented sequentially; all participants (including the patient) were instructed to listen to each segment, and then to immediately (within a few seconds) verbally recall that segment only. Participants were instructed to repeat what they had heard, not necessarily verbatim but in as much detail as possible.

Sentence Pairs: The sentence stimuli were composed of 12 “coherent” and 12 “incoherent” pairs of sentences. Coherent pairs of sentences shared a continuous context (e.g., both sentences would describe a continuous event happening in a classroom), whereas incoherent pairs of sentences have discontinuous contexts (e.g., one sentence might describe an event taking place on the ocean whereas the other sentence might describe an event happening in the subway). Participants listened to one pair of sentences at a time, and were instructed to repeat what they had heard verbatim. All sentences were between 8 and 13 words; for Coherent (Co) pairs, mean lengths were 10.3 words for the first sentence and 10.8 for the second sentence; for Incoherent (inCo) pairs, mean lengths were 10.6 words for the first sentence and 11.2 for the second sentence. See Supplementary Materials for the complete set of sentences.

Short Stories: The short story stimuli were composed of 4 “coherent” and 4 “incoherent” short stories. Each coherent story (Co) was a 2 min excerpt from a single story; each incoherent short story (inCo) was generated by concatenating two 1 min excerpts from two unrelated stories. For one of the incoherent stories, the first-half story was a repetition of the first-half of one of the coherent stories. All short stories were narrated by the same person (from the podcast *Escape Pod*; see [Supplementary Table 1](#) for details). Participants were instructed to repeat what they had heard, not necessarily verbatim but in as much detail as possible. Due to time limitations, D.A. listened to 3 coherent and 3 incoherent stories, whereas control participants listened to all 4 coherent and 4 incoherent stories.

Wechsler Memory Scale-IV Logical Memory Test: A narrative paragraph from WMS (“Anna Thompson”, 65 words) was used. Participants listened to the paragraph and were instructed to repeat what they had heard verbatim.

See [Supplementary Table 2](#) for detailed instructions for all tasks.

Scoring. Each participant’s verbal recall was scored using a

standardized protocol.

Long Story Segments: For each segment, memoranda (“details”) were defined by the experimenters for scoring purposes. The number of details recalled was recorded for each participant. The percentage of number of details recalled out of the total number of details was calculated for each participant.

Sentence Pairs: Each recall was given a score from 1 to 5 (5 = produced verbatim; 4 = 1–2 minor semantic and/or syntactic errors; 3 = a few semantic and/or syntactic errors; 2 = a trace of gist; 1 = complete failure).

Short Stories: For each short story, memoranda (“details”) were defined by the experimenters for scoring purposes (See Supplementary Materials). Transcriptions of participants’ recall were also broken into details. Each recalled detail was given a score (0–2) based on its degree of semantic overlap with the list of details in the original story (2 = complete semantic overlap; 1 = partial semantic overlap; 0 = no semantic overlap, repetitions, metacognitive statements, commentary, and confabulations). The final score was the sum of the scores for all the statements in the recall.

WMS: The WMS was scored in the manner prescribed by the scale. There are 25 pieces of information in the paragraph; a point was given for each piece of information recalled accurately.

2.3. fMRI tasks: auditory narrative listening

Auditory stimuli used for this study were generated from a 7 min real life story (*Pieman* narrated by Jim O’Grady, recorded at *The Moth*). In the Intact Story condition, participants listened to *Pieman* from beginning to end. In the Scrambled Paragraphs condition, *Pieman* was manually segmented into 12 paragraphs (mean duration 33.9 s; s.d. 20.6 s) and randomly temporally re-ordered to create the stimulus. Both the Intact Story and Scrambled Paragraphs stimuli were preceded by 12 s of music plus 3 s of silence, and followed by 15 s of silence, all of which were discarded from analyses. For control participants, attentive listening to the story was confirmed using a questionnaire after the scan. See [Simony et al. \(2016\)](#) for further details.

D.A. was scanned twice while listening to the *Pieman* Intact Story (data collected in 2015), and twice while listening to the Scrambled Paragraphs stimulus (data collected in 2018). All four scans were used in the analyses.

2.4. MRI acquisition

Control participants, data from [Simony et al. \(2016\)](#), were scanned at Princeton University in a 3 T full-body MRI scanner (Skyra; Siemens) with a 16-channel head coil. Functional images were acquired using a T2* weighted echo planar imaging pulse sequence (repetition time (TR) = 1500 ms; echo time (TE) = 28 ms; flip angle = 64°). Each volume comprised 27 slices of 4 mm thickness (in-plane resolution = 3 × 3 mm²; field of view (FOV) = 192 × 192 mm²). Slice acquisition order was interleaved. Anatomical images were acquired using a T1-weighted magnetization-prepared rapid-acquisition gradient echo (MP-RAGE) pulse sequence (TR = 2300 ms; TE = 3.08 ms; flip angle = 9°; resolution = 0.89 mm³; FOV = 256 × 256 mm²). All participants’ heads were stabilized with foam padding to minimize movement. Stimuli were presented using MATLAB Psychophysics Toolbox. Participants were provided with MRI compatible in-ear mono earbuds (Sensimetrics Model S14) to deliver the same audio input to each ear. MRI-safe passive noise-cancelling headphones were placed over the earbuds to attenuate the scanner noise.

The amnesic patient was scanned in two separate sessions. The Intact Story data were collected in 2015 at Rotman Research Institute in a 3 T full-body MRI scanner (Siemens). Functional images were acquired using a T2* weighted echo planar imaging pulse sequence (TR = 1500 ms; TE = 30 ms; flip angle = 75°). Each volume comprised 28 slices of 4 mm thickness (in-plane resolution = 3 × 3 mm²; FOV = 192 × 192 mm²).

Anatomical images were acquired using a T1-weighted MP-RAGE pulse sequence (TR = 2000 ms; TE = 2.63 ms; resolution = $1 \times 1 \text{ mm}^3$; FOV = $256 \times 256 \text{ mm}^2$; 160 slices).

The Scrambled Paragraphs data were collected in 2018 at University of Toronto in a 3 T full-body MRI scanner (Prisma; Siemens) with a 20-channel head coil. Functional images were acquired using a T2* weighted echo planar imaging pulse sequence (TR = 1500 ms; TE = 30 ms; flip angle = 75°). Each volume comprised 28 slices of 4 mm thickness (in-plane resolution = $3 \times 3 \text{ mm}^2$; FOV = $192 \times 192 \text{ mm}^2$).

The patient's head was stabilized with foam padding to minimize movement. Stimuli were presented using E-Prime. The patient was provided with MRI compatible in-ear mono earbuds (Sensimetrics Model S14) to deliver the same audio input to each ear. MRI-safe passive noise-cancelling headphones were placed over the earbuds to attenuate the scanner noise.

2.5. fMRI preprocessing

Control subjects' functional data were preprocessed and analyzed using FSL (www.fmrib.ox.ac.uk/fsl), including head motion and slice-acquisition time correction, spatial smoothing (6 mm FWHM Gaussian kernel), and high-pass temporal filtering (140 s period). Preprocessed data were transformed to a standard anatomical (MNI152) brain using FLIRT, and interpolated to 3 mm isotropic voxels.

Patient functional data were preprocessed using the same parameters as controls, with the following modifications. A patient lesion mask was created to identify the lesioned regions for exclusion from calculations of transformation to standard space, and from later analysis

(Supplementary Fig. 2). The mask was manually drawn on D.A.'s MP-RAGE anatomical image in native space. It was drawn liberally to exclude all affected areas. The lesion mask was used in conjunction with FSL nonlinear registration tools (FNIRT with option to ignore the masked region) to transform the patient's anatomical and functional data to standard MNI space and interpolated to 3 mm isotropic voxels.

2.6. Parcellation pattern similarity maps

We computed spatial pattern inter-subject correlation (pISC) (Chen et al., 2017; Nastase et al., 2019) in the Intact Story condition for each of 400 parcels from an independent whole-brain resting-state parcellation (Schaefer et al., 2018). Controls-vs-controls pISC was calculated in the following way. At each timepoint, the Pearson product-moment correlation coefficient was calculated between 1) one subject's BOLD activity spatial pattern (i.e., the vector of all voxel values) of a given parcel and 2) the BOLD activity spatial pattern averaged across all other subjects in the same parcel. This process was repeated for all subjects in a given condition and the resulting values were averaged across subjects and across timepoints to yield a single pISC value (the mean of the diagonal of the time-time correlation matrix). The controls-vs-controls Intact Story pISC values were plotted on the brain surface for every parcel (Fig. 2A) using NeuroElf (<http://neuroelf.net>). The map is displayed at a threshold of $r = 0.07$ for visualization purposes. We did not perform statistical thresholding for the controls-vs-controls Intact Story pISC map. As in other recent ISC papers (e.g., Chen et al., 2016; Baldassano et al., 2017), the initial thresholding of the within-condition ISC map serves to remove the noisiest (lowest reliability) voxels from the analysis, akin to the exclusion

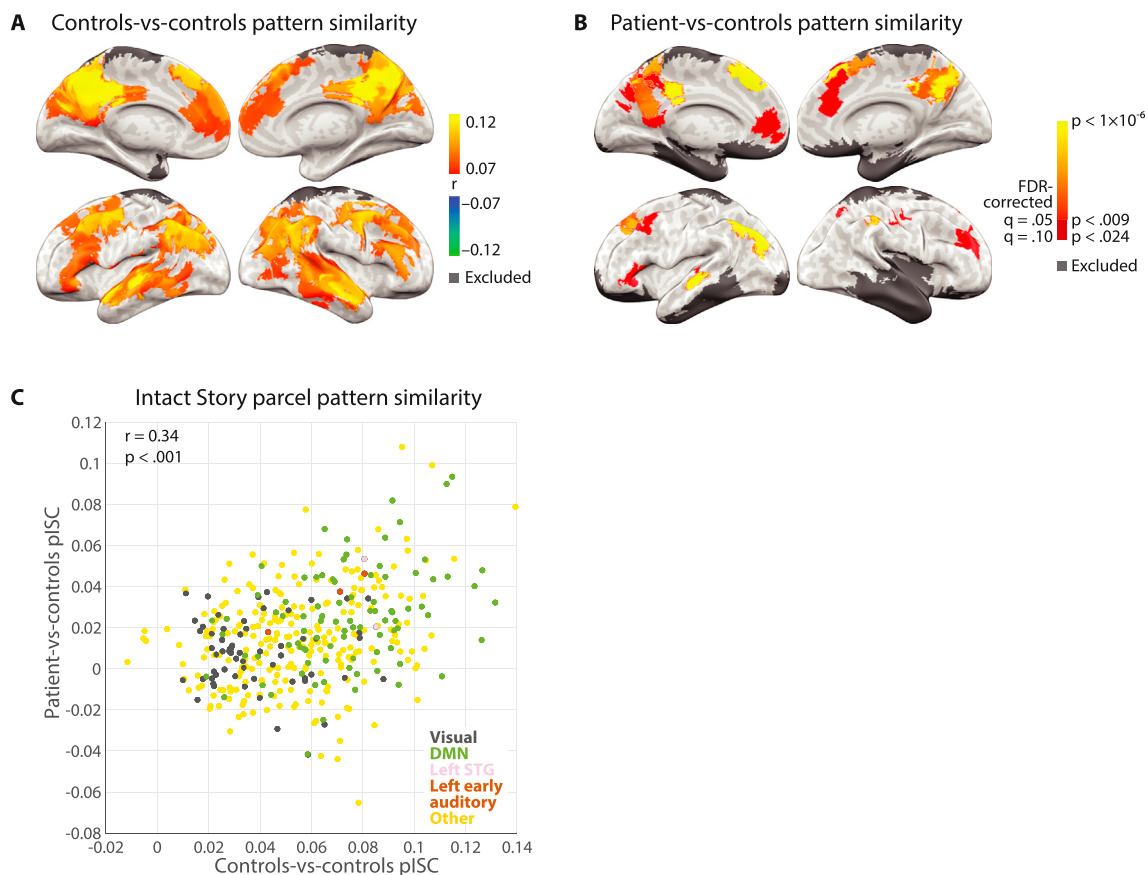


Fig. 2. Whole brain spatial pattern inter-subject correlation (pISC) maps of controls-vs-controls and patient-vs-controls in the Intact Story condition. **A)** Whole brain map showing regions where the highest within-group pattern similarity was observed among 36 control subjects, i.e., response reliability map. Threshold $r = 0.07$ for visualization purposes. **B)** Whole brain map showing regions where significantly similar pattern similarity was observed between the patient and control subjects; one-tailed p-values derived from permutation test and corrected for multiple comparisons across parcels using False Discovery Rate (FDR) with q criterion = 0.05 (orange to yellow) and q = 0.1 (red). **C)** Across parcels, pattern similarity distribution of patient-vs-controls was similar to that of controls-vs-controls ($r = 0.34$, $p < 0.001$).

of voxels with low signal-to-noise ratio. We chose an r threshold that approximates the temporal ISC-identified areas for Intact Story in Lerner et al. (2011).

We also calculated patient-vs-controls pISC for Intact Story. In order to preserve the temporal autocorrelation induced by the hemodynamics, functional data were first averaged in 8-TR (12 s) non-overlapping blocks. Next we correlated, for every block, each of the two patient functional runs with the average of $N-1$ control subjects, iterating over all possible combinations of $N-1$ control subjects and then averaging across the $N = 36$ combinations and across the two functional runs. This procedure matched the controls-vs-controls pISC procedure in that correlations were always calculated between one brain (the patient) and $N-1$ others ($36-1 = 35$ controls for the Intact Story condition). Null distributions were generated by randomly shuffling block-by-block pattern correlation matrices 10,000 times and retaining the mean diagonal value of each matrix (Kriegeskorte et al., 2008). As there were many parcels for which no null values exceeded the true pISC value, p -values (one-tailed) were estimated for all parcels by using the null distribution's mean and standard deviation to fit a normal distribution. We corrected for multiple comparisons across parcels by controlling the False Discovery Rate (FDR) (Benjamini and Hochberg, 1995) using q criterion = 0.05 (Fig. 2B, orange-yellow). Results are also shown at a lower q criterion of 0.1 (Fig. 2B, red). As the test of the patient's match to controls is predicated on there being an adequate signal in the control data, the patient-vs-controls map is masked with the pISC map of controls-vs-controls ($r > 0.07$).

We defined a BOLD threshold for excluding parcels with insufficient data. The threshold was set by creating a mean functional image across all conditions and all control subjects and identifying the approximate value (in this case 5000; this threshold may differ for different MRI machines or sequences) above which all remaining voxels fell within the brain. Voxels with values below this threshold, even though they might be within the brain, would be of no greater luminance than voxels falling

within the skull or even outside of the head or body, and thus could reasonably be considered regions of BOLD signal dropout. A control subject's data were retained for a given parcel if at least 50% of voxels in the parcel had mean (of the entire functional run) values above the threshold. As a result, some parcels, especially those near the edge of the brain and signal dropout regions, have a different number of control subjects contributing data. In control-vs-control pISC analyses, a parcel was retained if more than 50% of subjects' data were retained in that parcel (i.e., more than 18 subjects in the Intact Story condition). Of the 400 original parcels, 296 retained data from 100% of subjects and 387 retained data from more than 50% of subjects; thus 387 parcels were retained for controls-vs-controls maps. In patient-vs-controls pISC analyses, a parcel was retained if 1) more than 50% of control subjects' data were retained in that parcel; 2) at least 50% of voxels in the average patient data (average of 2 Intact Story functional runs and 2 Scrambled Paragraphs functional runs) pass the retention threshold; and 3) no more than 50% of the voxels in that parcel fell inside the experimenter-defined patient lesion mask. 349 parcels were retained for patient-vs-controls maps.

2.7. Regions of interest (ROIs) pattern similarity

Regions of interest (ROIs) were created by combining subsets of the parcels: left early auditory cortex, left superior temporal gyrus (STG), left posterior lateral parietal cortex (PPC), left posterior medial cortex (PMC), combined left medial prefrontal cortex (mPFC) and left dorsal medial prefrontal cortex (dmPFC), as well as combined right parahippocampal cortex (PHC) and temporal pole (see Supplementary Table 3 for a list of parcels used to create these ROIs).

pISC in these ROIs is shown in Fig. 3. Patient-vs-controls pISC and controls-vs-controls pISC were calculated in exactly the same manner as described above for parcels. Null distributions were generated by averaging the data in non-overlapping blocks of 8 TRs, calculating the block-

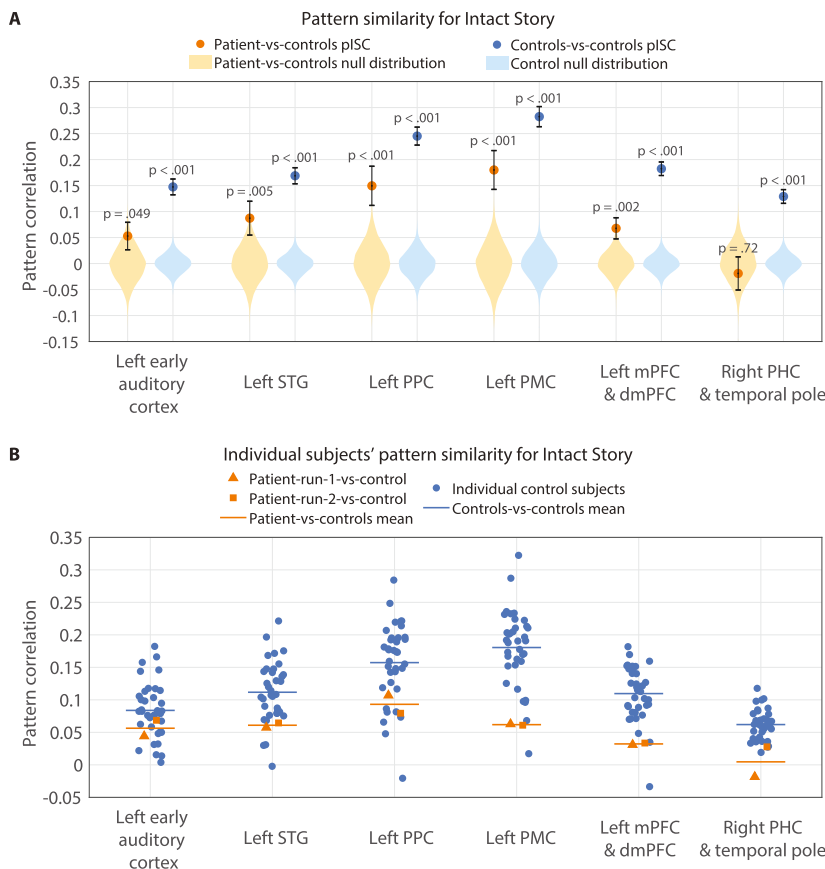


Fig. 3. Intact Story pattern similarity in a priori ROIs. **A)** Intact Story spatial pattern inter-subject correlation (pISC) in left early auditory cortex, left superior temporal gyrus (STG), left posterior lateral parietal cortex (PPC), left posterior medial cortex (PMC), combined left medial prefrontal cortex (mPFC) and dorsal medial prefrontal cortex (dmPFC), as well as combined right parahippocampal cortex (PHC) and temporal pole ROIs. To preserve temporal autocorrelation induced by the hemodynamics of BOLD signal, functional data were averaged in 8-TR (12 s) non-overlapping blocks before calculating pISC and null distributions. Null distributions were generated by calculating the block-by-block correlation matrix, randomly permuting this matrix 10,000 times, and retaining the mean diagonal value in each permutation. The mean diagonal values in the null are plotted as violin distributions for each ROI. The mean diagonal of the original blocked pattern correlation matrix is the true pISC value (plotted as a filled circle). **B)** Individual subjects' TR-by-TR pISC in each ROI. Note that the values here are different than those in Fig. 3A because the functional data are not block-averaged.

by-block correlation matrix, randomly permuting this matrix 10,000 times, and retaining the mean diagonal value of each matrix (see [Supplementary Fig. 3](#); [Kriegeskorte et al., 2008](#)). The mean diagonal values in the null were plotted as violin distributions for each ROI. The pISC value was defined as the mean of the diagonal of the original pattern correlation matrix (pISC is plotted as a filled circle).

Measurement error of the pISC values was computed using a bootstrapping approach. We generated a surrogate distribution of the mean pISC values containing 10,000 surrogate diagonals of the 8-TR block-averaged time-time pISC matrix to preserve the temporal autocorrelation induced by the hemodynamics. Each surrogate set of pISC values was generated by sampling the pISC values along the diagonal with replacement. The sampling was performed in blocks of 8 contiguous TRs (12 s) so that the surrogate distribution would preserve the temporal autocorrelation induced by the hemodynamics. After each surrogate set of pISC values was computed, the mean of that surrogate set was computed across all timepoints. The standard deviation of this distribution then provided the standard error of the mean (error bar on filled circles in [Fig. 3A](#)).

Comparison of pISC between groups was performed with two-tailed unpaired t-tests of the 36 patient-vs-controls to the 36 controls-vs-controls values, separately for early auditory cortex and STG, for Intact Story. Comparison of patient-vs-controls pISC between mPFC and PPC, and between mPFC and PMC, was performed with two-tailed unpaired t-tests of the 36 patient-vs-controls values for each ROI.

Individual control subject and individual patient functional run pISC values, calculated at the individual TR level, are shown in [Fig. 3B](#).

2.8. Unscrambling analyses

In order to compare Intact Story brain responses to Scrambled Paragraphs brain responses, it was necessary to re-order the Scrambled Paragraphs data such that the acoustic input would be matched at each timepoint across the two conditions. In other words, the Scrambled Paragraphs needed to be “unscrambled” to reconstruct the same ordering from the Intact Story.

We first manually identified (using Adobe Audition) the onset and offset of speech in the Intact Story and Scrambled Paragraphs stimuli, thus excluding pre-story music and post-story silence. We then identified boundaries of the 12 paragraphs in the Scrambled Paragraphs stimulus and the same boundaries in the original Intact Story stimulus. All boundaries were recorded with a temporal resolution of 44.1 KHz (0.002 s). As the BOLD data were collected at a 1.5 s TR resolution, paragraph boundaries did not necessarily fall at the beginning of a TR. To avoid the accumulation of small errors during the unscrambling procedure, we resampled the fMRI timecourses to a higher temporal resolution (50 Hz) to match the Intact and the Scrambled Paragraphs fMRI timecourses more precisely. To verify the beginning and end times of the auditory stimulus in the fMRI timecourse, the correlation was calculated between 1) each participant’s fMRI timecourse in the auditory cortex and 2) the audio envelope of the stimulus (both resampled to 50 Hz) at all possible lags to find the peak correlation. We shifted each participant’s fMRI time course to maximize the correlation with the audio envelope. This procedure corrects for the delay due to hemodynamic lag (near equivalent to shifting the fMRI time course by 3 TRs, or 4.5 s). We then “unscrambled” the fMRI timecourse of the Scrambled Paragraphs condition to match the temporal order of the Intact Story condition. The data (Intact Story and now “Unscrambled Paragraphs” conditions) were resampled back to the original frequency (1/1.5 Hz) for all subsequent analyses.

The critical question is whether the Unscrambled Paragraphs condition is significantly different from the Intact Story condition, i.e., whether subjects listening to the (Un)scrambled paragraphs version of the story are as similar to Intact Story listeners as Intact Story listeners are to each other. In other words, for a given brain region, did scrambling the story significantly affect brain responses? Thus the critical comparison is between 1) Intact Story pISC, and 2) Intact Story vs. Unscrambled

Paragraphs pISC. We sought to test whether these two were significantly different, first when calculating pISC between controls only, and second when calculating pISC between patient and controls.

Controls-vs-controls pISC and patient-vs-controls pISC for Intact Story calculations were described earlier (they appear in [Fig. 2](#)). Intact Story vs. Unscrambled Paragraphs pISC was calculated for controls-vs-controls in the same manner: at every TR, the spatial activity pattern of a subject in the Unscrambled Paragraphs condition was correlated with the average spatial activity pattern of a pseudo randomized combination of $N-1$ ($36-1 = 35$) subjects’ in the Intact Story condition. The mean diagonal of the time-time correlation matrix was retained; we iterated over all 18 Unscrambled Paragraphs subjects and averaged to obtain a single pISC value. This was performed for every parcel falling within the controls-vs-controls Intact Story reliability map ($r > 0.07$, from [Fig. 2A](#)). For patient-vs-controls, Intact Story vs. Unscrambled Paragraphs pISC was calculated in an analogous manner: the patient’s spatial activity pattern from one of the two Unscrambled Paragraphs runs was correlated with the Intact Story average of $N-1$ ($36-1 = 35$) control subjects, and the mean diagonal of the time-time correlation matrix was retained; we iterated over the 2 Unscrambled Paragraphs patient runs and averaged to obtain a single pISC value. This was performed for every parcel falling within the controls-vs-controls Intact Story reliability map (from [Fig. 2A](#)).

Between-condition comparisons of 1) Intact Story pISC, and 2) Intact Story vs. Unscrambled Paragraphs pISC, were calculated by generating surrogate distributions of the difference between conditions, using a bootstrapping approach (sampling 10,000 times with replacement). Each surrogate set of pISC difference values was generated by sampling the pISC values along the diagonal with replacement. After each surrogate set of pISC difference values was computed, the mean of that surrogate set was computed across all timepoints. This was performed for every parcel falling within the controls-vs-controls Intact Story reliability map ($r > 0.07$, from [Fig. 2A](#)) and FDR correction was performed within this mask. One-tailed p-values are plotted for each brain parcel in [Fig. 4A](#) (controls-vs-controls Intact Story > controls Intact Story vs. controls Unscrambled Paragraphs) and [Fig. 4B](#) (patient-vs-controls Intact Story > controls Intact Story vs. patient Unscrambled Paragraphs).

Two parcels which passed FDR correction in the patient-vs-controls Intact Story > controls Intact Story vs. patient Unscrambled Paragraphs analysis ([Fig. 4B](#)) are displayed in [Fig. 4C](#): the mean patient-vs-controls Intact Story pISC and Intact Story vs. Unscrambled Paragraphs pISC, as well as the pISC value for each of the two contributing patient runs. This display merely serves to visualize the data which went into the brain-wide parcel map analysis; it is not a different statistical test from the FDR-corrected test shown in [Fig. 4B](#).

As with the parcels above, comparisons of Intact Story and Unscrambled Paragraphs were performed in a priori ROIs: Left early auditory cortex, left PPC, left PMC, combined left mPFC and dmPFC, left STG, combined right PHC and temporal pole, right PPC, right PMC, and right mPFC ([Supplementary Fig. 4](#)). pISC measurement error was calculated using the same 8-TR block bootstrap approach as for [Fig. 3A](#). Between-condition comparisons of pISC in [Supplementary Fig. 4](#) were calculated by generating surrogate distributions of the difference between conditions, using a bootstrapping approach (sampling 10,000 times with replacement) and the same blocking parameters as above. One-tailed p-values are reported.

For within-patient Intact Story vs. Unscrambled Paragraphs analyses, see [Supplementary Fig. 5](#).

2.9. Patterns across time

Controls-vs-controls and patient-vs-controls pISC were examined at individual timepoints and time bins across the duration of the Intact Story. TR-by-TR pISC is displayed for the left auditory cortex and left PPC ROIs ([Fig. 5A & B](#)). For coarser time bin analysis, bins were created by evenly dividing the Intact Story into three segments and averaging TR-by-TR pISC across time within each segment ([Fig. 5C & D](#), left panels).

pISC measurement error for the segments was calculated using the same block bootstrap approach as for Fig. 3A, but with blocks of 9 TRs instead of 8 TRs to be divisible by the 90-TR segments. Comparison of whether the difference between controls-vs-controls and patient-vs-controls pISC changed across the segments was conducted with two-tailed unpaired t-tests of the difference.

To examine the temporal specificity of pISC, we computed voxel pattern lag correlation timecourses by calculating the pISC of controls-vs-controls and of patient-vs-controls at every possible temporal offset (e.g., time lag = 1 TR, 2 TRs, etc.) from -30 to +30 TRs (Fig. 5C & D, right panels). This procedure requires that TRs with no corresponding data between conditions be removed from analysis; e.g., at lag = +30 TRs, the patient data and control data are offset by 30 TRs, and thus 30 TRs are dropped from the beginning of one data series and another 30 TRs are dropped from the end of the other data series.

2.10. Pattern vs. temporal ISC

Spatial pattern inter-subject correlation (pISC) and temporal inter-subject correlation (tISC) were calculated for every parcel in the brain using the Intact Story data, both for controls-vs-controls and for patient-vs-controls, and visualized in scatter plots (Supplementary Fig. 6). Visual and default mode networks refer to a standard 7-Network resting-state parcellation (Schaefer et al., 2018; Yeo et al., 2011). Auditory parcel selection is described above in Methods: Regions of interest; see also Supplementary Table 3.

3. Results

3.1. D.A. Displays behavioral patterns of anterograde amnesia in tests of verbal recall

As the goals of the current experiment are to investigate default network activity in the absence of a functioning hippocampus, we first

sought to establish that D.A. displays behavioral patterns concomitant with severe bilateral hippocampal damage, i.e., anterograde amnesia: impaired but not absent immediate prose recall, catastrophic memory loss after a filled delay, performance disruption from discontinuity (e.g., topic changes), and preserved short-term memory when active rehearsal is allowed (Squire and Wixted, 2011). Rosenbaum et al. (2008) previously reported that D.A. has dense anterograde amnesia, e.g., <1st percentile on delayed memory tasks in the Wechsler Memory Scale (WMS; Wechsler, 1987). Here we extend these prior findings with additional tests of immediate verbal recall. To probe his comprehension of semantically-rich material, we constructed tests using sentences and narratives of different lengths and coherence. D.A. and controls participated in four immediate verbal recall tasks: WMS, Long Story Segments, Short Stories, and Sentence Pairs (Fig. 1B).

The WMS Logical Memory test (Wechsler, 1987) is a common measure of “prose” recall in amnesic patients (e.g., Baddeley and Wilson, 2002; Kopelman, 1987; Rosenbaum et al., 2008). In this test the experimenter reads aloud a 65-word story, and the patient is then asked to repeat it verbatim. D.A. recalled 9 out of a possible 25 items from the story Fig. 1B). This value was lower than all of the age-matched controls, second-lowest amongst the younger controls, and is typical for amnesic individuals (ranges observed by Baddeley and Wilson, 2002, for three groups: amnesics, 50-years-old controls, and 70-years-old controls, are reproduced in the WMS panel of Fig. 1B). There was no statistical difference between D.A.’s recall performance and that of controls’ using Crawford and Howell (1998) single-case t-test ($t(13) = -1.33, p = 0.21$).

To test the limits of more natural and extended narrative comprehension in amnesia, we also measured D.A.’s verbal recall for longer narratives. In the Long Story Segments task, auditory stories of 5 and 8 min were played 1 min at a time. After each such segment, all participants were asked to repeat what they had heard, not necessarily verbatim but in as much detail as possible. D.A.’s performance on this test was poor (Fig. 1B) but not statistically different from controls ($t(11) = -1.21, p = 0.25$).

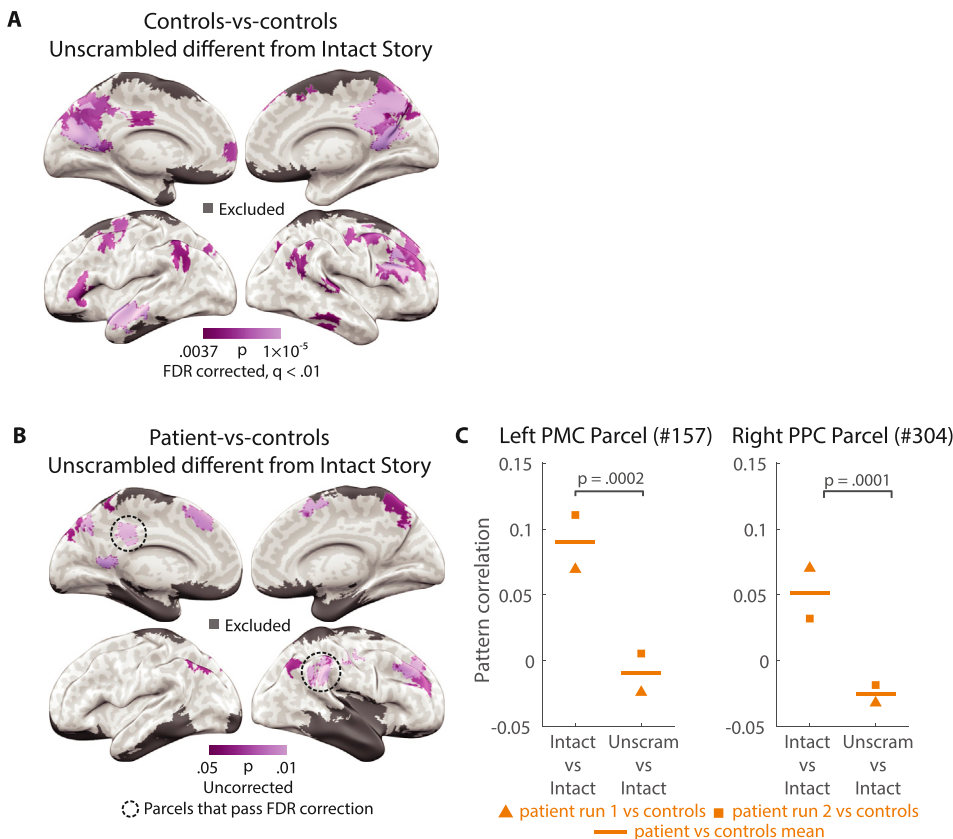


Fig. 4. Unscrambling analysis. A) Parcels for which pattern correlation of controls-vs-controls Intact Story was higher ($p < 0.01$) than controls Intact Story vs. controls Unscrambled Paragraphs. Map masked with controls-vs-controls Intact Story reliability (pISC) $r > 0.07$. B) Parcels for which pattern correlation of patient-vs-controls Intact Story was higher ($p < 0.05$) than patient Unscrambled Paragraphs vs. controls Intact Story. Map masked with controls-vs-controls Intact Story reliability (pISC) $r > 0.07$. The two parcels circled in black dotted lines passed False Discovery Rate (FDR) correction. C) Two parcels which passed FDR correction in the patient-vs-controls Intact Story > controls Intact Story vs. patient Unscrambled Paragraphs analysis from Fig. 4B. The mean patient-vs-controls Intact Story pISC (left) and the mean controls Intact Story vs. patient Unscrambled Paragraphs pISC (right, horizontal lines), as well as the pISC value for each of the two contributing patient runs of Scrambled Paragraphs (square and triangle markers). This display merely serves to visualize the data which went into the brain-wide parcel map analysis; it is not a different statistical test from the FDR-corrected test shown in Fig. 4B.

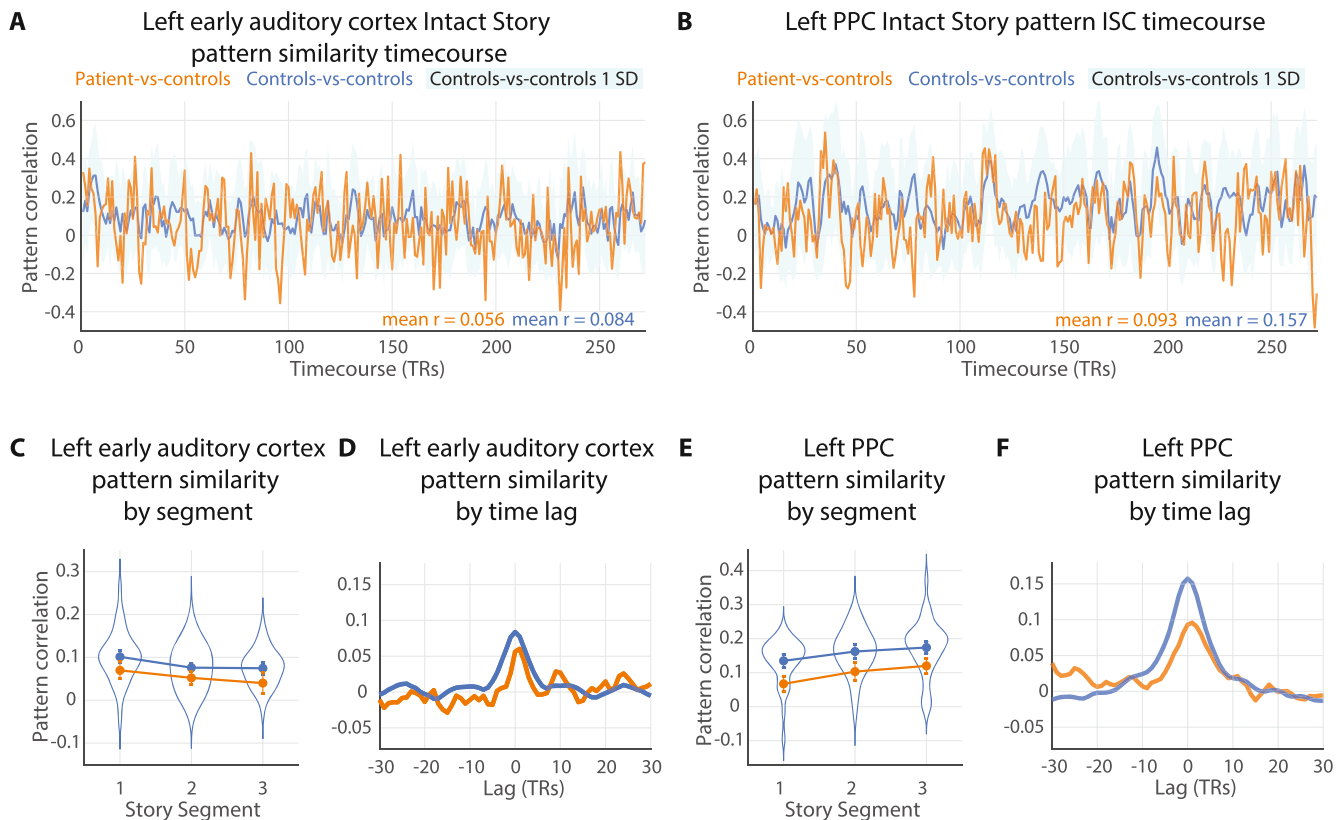


Fig. 5. Pattern similarity (pISC) across time. **A & B**) Patient-vs-controls and controls-vs-controls spatial pattern inter-subject correlation (pISC) in left early auditory cortex and left posterior lateral parietal cortex (PPC) at every timepoint of the Intact Story. Standard deviation of controls-vs-controls at each timepoint plotted in light blue. Mean values of each pattern similarity timecourse printed in lower right corner. **C & E**) The Intact Story data were evenly divided into three segments (90 TRs or 135 s per segment) and TR-by-TR pISC was averaged for each segment, in patient-vs-controls and controls-vs-controls comparisons. Individual subjects' average pISC within each 1/3-story segment were plotted as violin distributions. Error bars represent the standard deviation of 8-TR block-bootstrapped subject-average pISC to preserve temporal autocorrelation induced by hemodynamics. **D & F**) pISC lag correlation of patient-vs-controls and controls-vs-controls in left early auditory cortex and left PPC. The peaks at lag zero, with gradual declines as lag magnitude increases (either negative or positive), indicate that the pattern match between patient-vs-controls (orange) and controls-vs-controls (blue) was temporally specific, i.e., dependent on the stimulus matching moment-by-moment.

We next examined narrative recall while manipulating the coherence or incoherence of the narrative. In the Short Stories task, “coherent” auditory stories were created by excerpting 2 min from a single story (*Co*), and “incoherent” stories generated by concatenating two 1 min excerpts from two unrelated stories (*inCo1* and *inCo2*). Again, the patient and controls were asked to repeat what they had heard, not necessarily verbatim but in as much detail as possible. D.A.’s performance on this test was poor (Fig. 1B) but not statistically different from controls (coherent stories: $t(11) = -1.74$, $p = 0.11$; incoherent stories: $t(11) = -1.72$, $p = 0.11$). Notably, when incoherent stories were scored separately for the first and second half (*inCo1* and *inCo2*), D.A.’s performance was near the mean of controls for the second halves of stories, but he recalled only one gist-like detail from the first half of any of the incoherent stories. Here, the discontinuity introduced by the concatenation of two different stories may have impacted D.A.’s ability to retrieve the material from before the discontinuity (event boundary) that occurred 1 min earlier. Unfortunately, it was not possible to score coherent stories separately for the first and second half, as D.A.’s (and many controls subjects’) verbal reports were largely gist-like, and thus very few of the recall statements could be clearly identified as coming from the first or second half of the coherent story. Comparing his memory for the full coherent stories separately to the first and second halves of the incoherent stories, we found that D.A.’s performance was significantly worse on the first halves of incoherent stories compared to the coherent stories ($t(4) = 4.77$, $p = 0.009$), whereas there was no difference between the second halves of incoherent stories relative to coherent stories ($t(4) = 1.11$, $p = 0.33$).

We also assessed recall for shorter linguistic sequences. On each trial of the Sentence Pairs task, participants listened to two consecutive

sentences (each sentence composed of 8–13 words) and then immediately attempted to repeat verbatim what they had heard. D.A.’s performance was not different from that of controls for either “coherent” sentence pairs (when the two sentences described a continuous context; $t(13) = 0.005$, $p = 0.996$) or for “incoherent” sentence pairs (when the two sentences described different contexts; $t(13) = -1.15$, $p = 0.27$). D.A.’s performance was close to the mean of controls for coherent sentence pairs and poor (3rd lowest) for incoherent sentence pairs (Fig. 1B). D.A.’s recall of coherent sentence pairs was significantly better than his recall of incoherent sentence pairs ($t(46) = 2.74$, $p = 0.009$). These results converge with studies of hippocampal amnesics showing that prior knowledge can improve short-term memory retention for sentences (Race et al., 2015b).

After the first scan session (described below), and several minutes after D.A. had exited the MRI machine, the experimenter asked D.A. whether he remembered anything from the auditory narrative he had listened to inside the scanner. D.A. could not verbalize any accurate memory for content from the story; he made only statements that were either so vague as to be indistinguishable from guesses, or completely incorrect, even when prompted with several story details (see Supplementary Materials for a transcript of the interview).

Taken together, D.A.’s behavior patterns match those of anterograde amnesic syndrome arising from severe bilateral hippocampal damage. He demonstrated preserved immediate recall of short sentences (coherent Sentence Pairs), and impaired recall of even very recent (a few seconds ago) material prior to discontinuities introduced by an unrelated sentence (incoherent Sentence Pairs). His immediate verbal recall performance was poor but within the range of control participants. For two

tests, 1) recall of coherent Sentence Pairs, and 2) recalling the second half of an Incoherent Story, his performance was close to the mean of controls. D.A.'s prose and narrative immediate recall were poor but not completely absent (WMS, Long Story Segments, coherent Short Stories), comparable to scores previously reported for amnesics and age-matched controls; and he had virtually no memory of events prior to a discontinuity 1 min earlier (incoherent Short Stories). D.A.'s impairments on immediate recall of narrative information may underestimate his ability to retain semantically coherent information over time, because the transition from listening to answering is itself a major event boundary which causes a partial loss of information prior to the boundary.

3.2. D.A.'s neural responses to an auditory narrative match the responses of controls (Intact Story Match)

The primary question of the study was whether cortical regions of the default network would exhibit long-timescale properties even in the absence of an intact hippocampus. In neurotypical subjects the activity patterns of default network areas for each paragraph in a continuous story depend on the content presented in prior paragraphs (Hasson et al., 2015; Lerner et al., 2011). If information from the prior paragraph is not being carried forward into the current paragraph in the patient's brain, the patient's default network activity pattern for each paragraph should be different from the neurotypical pattern. In other words, if default network regions can integrate information across paragraphs without the hippocampus, then amnesic default network activity patterns should match controls above chance when listening to the intact story. To test this, we compared brain activity between the patient and control participants as they listened to the same intact 7 min auditory narrative. Note that the patient does have residual hippocampal tissue—less than $\frac{1}{3}$ of the left hippocampus remains—but 1) he presents behaviorally as densely amnesic, and 2) meta-analysis of non-human primate data shows that partial hippocampal loss can be equivalent or worse to more severe damage in terms of its impact on delayed memory performance (Baxter and Murray, 2001).

First, we established the regions where control participants exhibited similar brain activity patterns with each other while listening to the intact narrative by calculating pattern similarity in every parcel (Schaefer et al., 2018) across the brain. Previous fMRI studies of the temporal integration hierarchy have largely used temporal ISC (tISC; e.g., Hasson et al., 2008; Lerner et al., 2011; Simony et al., 2016); here we use spatial pattern ISC (pISC; e.g., Chen et al., 2017; Oedekoven et al., 2017; Baldassano et al., 2018; Nastase et al., 2019) which allows estimates of response reliability to be calculated at each TR. The two are closely related but not redundant (Nastase et al., 2019; Supplementary Fig. 5). We calculated pattern similarity for controls-vs-controls at every TR of the Intact Story and averaged across all TRs within each parcel (Fig. 2A). In agreement with prior studies, the spatial patterns of neural responses were similar between control subjects in widespread regions, ranging from early auditory areas, to linguistic areas, to default network areas including posterior medial cortex (PMC), lateral posterior parietal cortex (PPC), and medial prefrontal cortex (mPFC) (Chen et al., 2017; Baldassano et al., 2018; Nastase et al., 2019). Controls-vs-controls whole-cortex response reliability map (Fig. 2A) is shown at $r > 0.07$ for visualization purposes. Note that these comparisons should not be interpreted as a comparison of the spatial extent of above-threshold pISC between controls and patient; the controls-vs-controls map is not statistically thresholded, and the patient-vs-controls map is masked with the controls-vs-controls map, thus precluding interpretations of spatial extent.

Next, we compared the patient's moment-by-moment brain activity to that of control participants as they listened to the same Intact Story. Mirroring the analysis above, we calculated pattern similarity for patient-vs-controls at every timepoint of the Intact Story and averaged across all timepoints within each parcel (Fig. 2B), masked with the controls-vs-controls whole-cortex response reliability map. For statistical reasons,

this analysis was performed in 8-TR bins; see Methods. Brain responses of the amnesic patient were similar to responses in neurotypical control subjects in many cortical areas, including early auditory areas, bilateral PMC, bilateral PPC, and bilateral mPFC. Note that the patient's more severe damage is in the right hemisphere temporal lobe. Whole-cortex maps show one-tailed p-values derived from permutation test and corrected for multiple comparisons using FDR with q criterion = 0.05 (orange-yellow). Parcels passing a more lenient threshold of $q = 0.1$ are also displayed (red).

To compare controls-vs-controls and patient-vs-controls distributions of pattern similarity across the brain, we visualized pattern similarity of individual parcels in a scatter plot (Fig. 2C). Across parcels, the pattern similarity of patient-vs-controls was significantly similar to that of controls-vs-controls ($r = 0.34$, $p < 0.001$). We also evaluated this relationship when restricting to a higher threshold, as parcels with very low correlations might be considered noise. Using a threshold of $r > 0.07$ for controls-vs-controls and $r > 0.03$ for patient-vs-controls, 55 parcels were retained, and the correlation of pattern similarity across parcels between patient-vs-controls and controls-vs-controls was $r = 0.31$, $p = 0.02$.

3.3. Significant similarity of neural patterns between patient and controls in default network ROIs (Intact Story Match)

Our main interest was in default network regions, which were previously shown to integrate information over long timescales during continuous natural input, such as movies and stories (Hasson et al., 2008; Lerner et al., 2011; Simony et al., 2016; Chen et al., 2016). Thus, we examined pattern similarity in three default network ROIs (PPC, PMC, mPFC), as well as in (i) early auditory cortex and (ii) a larger superior temporal gyrus (STG) ROI that included early auditory cortex. As the patient's brain damage is most severe in the right hemisphere (including volume loss in right-hemisphere cortical areas outside of the MTL), ROI analyses were restricted to the left hemisphere, with the exception of a control region in the right anterior temporal and parahippocampal cortex where there is little tissue remaining. For each ROI, pattern similarity was calculated for controls-vs-controls and for patient-vs-controls at every 8-TR block of the Intact Story and averaged across all blocks (same analysis as conducted for each parcel in Fig. 2). A null distribution was created for each ROI by randomly permuting the block-by-block pattern correlation matrices (Supplementary Fig. 3) and recalculating the mean diagonal 10,000 times.

We expected auditory cortex activity patterns to be similar across patients and controls, as these areas respond primarily to immediate acoustic features of the auditory narrative. This prediction was confirmed: the true patient-vs-controls pattern similarity value was positive and well outside the null distribution for both the early auditory cortex ($M = 0.053$, $p = 0.049$) and STG ($M = 0.087$, $p = 0.0052$) (Fig. 3A). Controls-vs-controls pattern similarity was also significant in these two regions (early auditory: $M = 0.15$, $p < 0.001$; STG: $M = 0.17$, $p < 0.001$) and higher than patient-vs-controls pattern similarity (early auditory: $t(70) = 8.89$, $p < 0.001$; STG: $t(70) = 8.00$, $p < 0.001$; Fig. 3A). These data suggest that fMRI signal in the control data is more reliable overall, possibly due to the lower age of the control participants (Campbell et al., 2015) or other idiosyncrasies of the patient testing. Nonetheless, the statistically above-chance match between patients and controls is positive evidence of a common response between amnesic and neurotypical brains.

In PPC, PMC, and mPFC, default network regions which were previously shown to integrate information over long timescales, we observed similar activity between patient and controls (Fig. 3A), with the true correlation values positive and falling well outside of the null distributions (PPC: $M = 0.15$, $p < 0.001$; PMC: $M = 0.18$, $p < 0.001$; mPFC: $M = 0.068$, $p = 0.0016$). In mPFC the match between patient and controls was weaker than in PPC and PMC (mPFC vs. PPC: $t(70) = 130.1$, $p < 0.001$; mPFC vs. PMC: $t(70) = 175.8$, $p < 0.001$). In all three of these default network ROIs, controls-vs-controls pattern similarity was significantly

positive (PPC: $M = 0.25$, $p < 0.001$; PMC: $M = 0.28$, $p < 0.001$; mPFC: $M = 0.18$, $p < 0.001$), as observed in prior studies (Chen et al., 2017; Baldassano et al., 2018).

In right PHC and temporal pole, a severely damaged region of the patient's brain, the true patient-vs-controls correlation fell inside the null distribution ($M = -0.019$, $p = 0.72$), i.e., there was no similarity effect. This is as expected given that virtually no BOLD signal was detectable in this area. This ROI normally shows positive pattern similarity between individuals during narrative listening, as demonstrated in the controls-vs-controls comparison ($M = 0.13$, $p < 0.001$; Fig. 3A).

Data for individual subjects in all ROIs are shown in Fig. 3B.

Altogether, the results in Figs. 2 and 3 show that patterns of activity during Intact Story listening were similar between the patient and controls across the brain. This was true for a number of individual parcels and a priori default network ROIs, and the overall distribution of patient-vs-controls pattern similarity strength across parcels mirrored that of the control subjects. Because the activity patterns of default network areas for each paragraph in a continuous story depend on the content presented in prior paragraphs in neurotypical subjects (Lerner et al., 2011; Hasson et al., 2015), these results suggest that default network regions can, to some extent, integrate information across paragraphs without an intact hippocampus. However, the match between patient and controls was weaker overall than the match of controls to each other. While this could be due to the patient being older than controls or other idiosyncrasies of the patient brain, it is also possible that default network patterns reflect a mixture of long- and shorter-timescale information, and the preserved component of the patient's default network activity pattern corresponded to shorter-timescale information; the Intact Story condition alone cannot conclusively exclude this interpretation. Thus, we examined the Scrambled Paragraphs condition of the experiment.

3.4. Default network responses affected by paragraph scrambling, even in absence of the hippocampus (Unscrambling and Scramble Reliability)

In prior studies, default network regions were shown to be able to integrate information across paragraphs, on the scale of 30 s or more, during continuous narrative processing. This was demonstrated in two complementary ways: 1) comparing Intact Story timecourses to "unscrambled" Scrambled Paragraphs timecourses, which showed that if the preceding paragraph was altered, then default network responses to the current paragraph were altered (Lerner et al., 2011); and 2) calculating temporal ISC for a Scrambled Paragraphs narrative, which showed that default network inter-subject response reliability was reduced when paragraph-level (or an equivalent window of time for visual stimuli) information was disrupted (Chen et al., 2016; Hasson et al., 2008; Honey et al., 2012; Lerner et al., 2011; Simony et al., 2016). By contrast, early auditory areas exhibit high inter-subject response reliability regardless of scrambling. We sought to replicate these effects in the current dataset, both in controls and in the patient, by comparing brain responses during Intact Story to those recorded during Scrambled Paragraphs.

First, we "unscrambled" the Scrambled Paragraphs brain data by identifying the TRs corresponding to each paragraph and re-ordering these to match the Intact Story. This created an "Unscrambled Paragraphs" version of the data in which each TR was time-aligned to the Intact Story, i.e., the same moment of the stimulus was presented for each TR of both conditions. Then, for each parcel of the brain, we calculated spatial pattern correlations between Unscrambled Paragraphs and Intact Story and tested whether this value was significantly different from pattern similarity between subjects listening to the Intact Story (the theoretical ceiling of response reliability). The unscrambling analysis confirmed that, in controls, default network regions such as PPC, PMC, and mPFC produced responses that did depend on the content of preceding paragraphs (map FDR corrected at $q < 0.01$), while low-level regions, e.g., early auditory cortex, produced responses that did not depend on prior paragraphs (Fig. 4A).

Importantly, two parcels in the patient-vs-controls comparison passed

FDR correction of $q < 0.05$: one in left PMC ($p = 0.0002$), and one in right PPC ($p = 0.0001$) (157 and 304 in the Schaefer et al., 2018 atlas), areas typically identified with the default network. The map in Fig. 4B is shown uncorrected at $p < 0.05$ in order to show where near-threshold parcels fall. Details of results from the two significant parcels are displayed in Fig. 4C.

In a priori ROIs, we observed significant effects of scrambling (unscrambled-vs-intact less correlated than intact-vs-intact) in left-hemisphere PPC, PMC, and mPFC for controls-vs-controls (PPC: $p = 0.0001$; PMC: $p = 0.0003$; mPFC: $p = 0.002$); and trends for the same effect in PPC ($p = 0.07$) and PMC ($p = 0.08$), but not mPFC ($p > 0.1$), for patient-vs-controls (Supplementary Fig. 4). Scrambling did not alter response patterns in early auditory cortex for either controls-vs-controls or for patient-vs-controls (Supplementary Fig. 4A, $ps > 0.1$). While two parcels in PPC and PMC passed the map-wide FDR-correction threshold of $q < 0.05$, the same test in the a priori left PPC and PMC ROIs was marginal ($p < 0.1$). This discrepancy is likely due to the much larger size of the a priori ROIs, as well as the fact that the significant PPC parcel was in the right hemisphere while the a priori PPC ROI was in the left hemisphere (selected due to the patient's MTL damage being less extensive on the left).

Second, we examined reliability (spatial pattern similarity) in the Scrambled Paragraphs condition for controls-vs-controls and patient-vs-controls. Echoing previous studies using temporal ISC with neurotypical subjects (Lerner et al., 2011; Simony et al., 2016), inter-subject pattern similarity strength in PPC and PMC was reduced by paragraph scrambling in the controls-vs-controls comparisons (PPC: $p = 0.08$; PMC: $p = 0.006$); we observed a similar pattern in the amnesic-vs-controls comparisons (PPC, $p = 0.002$; PMC, $p = 0.01$); but not in mPFC (Supplementary Fig. 4). As predicted, inter-subject pattern similarity strength in these auditory areas was unaffected by paragraph scrambling.

It should be noted that the patient MRI data for the two conditions were collected three years apart and using different scanners. Is it possible that between-condition effects could be driven by these differences rather than the manipulated experimental conditions? One data point that may help alleviate the concern is as follows: if Scrambled Paragraphs (collected 3 years later) had much lower signal quality than Intact Story, one would expect lower-level areas to have reduced reliability. However, we do not see evidence of this in auditory cortex or STG; in fact, in these regions the patient is (numerically) more similar to controls for the Scrambled Paragraphs condition than for the Intact Story. See Supplementary Figs. 4A and 4E: compare patient's values for II to IU, i.e., horizontal orange lines.

In sum, we observed that scrambling at the level of paragraphs affected the amnesic's default network responses in two ways: 1) the unscrambling analysis showed that if the preceding paragraph was altered, then default network responses to the current paragraph were altered; and 2) response reliability, measured using pattern similarity at each TR, was reduced when paragraph-level information was disrupted by scrambling. These results support the interpretation that the amnesic's default network regions were able to integrate information across paragraphs during the intact story, even in the absence of an intact hippocampus.

3.5. Patient-vs-controls neural pattern similarity is sustained across the duration of the story

While the above analyses examined whether the brain activity of the patient and controls was similar on average across all moments of the Intact Story, it was also important to test whether the similarity persisted across the full duration of the stimulus. Potentially, the patient could resemble controls most strongly at the beginning of the story, with similarity decreasing over time as the patient's memory of more distant prior information weakened.

Thus, we visualized pattern similarity, TR-by-TR, in left auditory cortex and left PPC (Fig. 5A and B). In both regions, more timepoints

were positive than negative (as should be expected given the positive means reported in Fig. 2A), for both patient-vs-controls (orange bars) and controls-vs-controls (blue lines). Note that, while the correlation magnitudes are comparable between the patient-vs-controls (orange bars) and controls-vs-controls (blue lines), the measurement precision is different across the two curves. This is because patient-vs-controls values reflect an average of 2 samples while the controls-vs-controls values reflect an average of 36 samples. See Supplementary Fig. 7 for timecourses in all a priori ROIs.

The similarity between patient and controls did not decrease over time in PPC (Fig. 5). We computed the average pattern similarity across the first third, middle third, and final third of the story. In auditory cortex, the correlation values numerically decreased slightly over time in both patient-vs-controls (orange) and controls-vs-controls (blue) (Fig. 5C). In any region, such a decrease might be due to either fatigue, or to properties of the stimulus that varied across segments of time—e.g., in auditory cortex, one segment might have lower volume variability than another and thus lower signal to drive ISC. Note that, despite the drop over time in auditory cortex, the *difference* between controls-vs-controls and patient-vs-controls remained constant ($p_s > 0.3$). In PPC, where one might have expected a decrease in patient-vs-controls over the duration of the story, there was no such drop (Fig. 5E). Numerically, both patient-vs-controls and controls-vs-controls pattern similarity actually increased across thirds of the story. Again, the *difference* between controls-vs-controls and patient-vs-controls remained constant ($p_s > 0.4$). These results are consistent with the interpretation that the patient's comprehension of the narrative was similar to controls even toward the later periods of the story.

To confirm that the pISC values reflected time-locked responses to the auditory narrative, we also evaluated the temporal precision of the match between patient and controls. Fig. 5D,F shows the pattern similarity lag correlation of patient-vs-controls and controls-vs-controls in auditory cortex and PPC. The peaks at lag zero, with gradual declines as lag magnitude increases (either negative or positive), indicate that the pattern match between patient-vs-controls (orange) and controls-vs-controls (blue) was temporally specific, i.e., dependent on the stimulus matching moment-by-moment.

4. Discussion

Default network areas are proposed to carry slowly-changing information during continuous semantically-rich input such as stories and conversation (Hasson et al., 2015). In healthy people, these areas are functionally coupled to the hippocampus and may work together to accumulate, maintain, and integrate information across time during naturalistic input (Chen et al., 2016). However, it is an open question whether the long-timescale capability of default network regions depends critically on interactions with the hippocampus. In this study we investigated whether default network areas can integrate information over tens of seconds even *without* an intact hippocampus by recording the brain activity of an amnesic patient with severe bilateral hippocampal damage as he listened to a 7 min auditory story. We observed that in some default network regions, including lateral posterior parietal cortex (PPC), posterior medial cortex (PMC), and medial prefrontal cortex (mPFC), there were significantly similar brain activity patterns between the amnesic and controls across the duration of the intact story, suggesting that at least some temporal dependencies at the timescale of paragraphs existed even without the support of an intact hippocampus. Furthermore, in both the patient and in neurotypical subjects, activity patterns in some default network areas (PPC and PMC, but not mPFC) for a given paragraph were changed if the preceding paragraph was changed (by scrambling the order of paragraphs), supporting the notion that these brain areas carried information across 30 s or more. In contrast, scrambling paragraph order did not affect early auditory areas in either the amnesic or neurotypical subjects. This study provides novel evidence that the purported ability of default network cortical areas to integrate

information across long timescales does not depend solely on interactions with the hippocampus.

How long are the long timescales of the default network? Several experiments have used parametrically scrambled narratives, both auditory and visual, to show that temporal activity profiles in default network areas were contingent on narrative segments being intact on the scale of 30 s or more (Hasson et al., 2008; Lerner et al., 2011; Honey et al., 2012). Windows longer than 30 s have not been tested with the scrambling method. In Chen et al. (2016), healthy subjects viewed movie events whose comprehension depended on prior events viewed either 1) several minutes earlier within the same continuous viewing session (i.e., without major interruption) or 2) a day earlier (introducing a major interruption). The day-earlier condition differentially recruited hippocampus and evinced strong stimulus-locked functional connectivity between the hippocampus and cortical default network areas, suggesting that hippocampus-default network interaction was important for bridging the discontinuity. Furthermore, default network response timecourses between the groups were initially dissimilar and eventually converged after 3–4 min, but post-viewing comprehension scores were indistinguishable between the groups. One interpretation of this result is that in the day-earlier condition, default network activity was altered by interactions with the hippocampus (greater demands on retrieval), while in the continuous condition, default network regions were able to support story comprehension with less or no hippocampal interaction due to their intrinsic retention of prior event information from minutes earlier. In other words, it took 3–4 min for the day-earlier group to retrieve and reload information to the default network so that they matched the continuous group. In actuality, the context-sensitivity of default network regions may be better described as a “preferred range” rather than an exact number of seconds; the measured range depends somewhat on the story being used, as different stories have different information density. For example, Lerner et al. (2014) showed that default network brain responses closely track the story stimulus even if it is presented temporally stretched and compressed, up to a point (200% stretching and 75% compression). All of these experiments were conducted in neurologically healthy individuals, and thus could not answer the question of whether the hippocampus is necessary for the long-timescale properties of default network regions.

While our results suggest that default network cortical areas are capable of supporting at least some online processing and comprehension of real-world events without an intact hippocampus, this does not contradict the view that default network-hippocampus interactions are needed for encoding and later retrieval of the event information from long-term memory. Regardless of their online processing abilities, hippocampal amnesics are unable to retrieve episodic information at a later time, either due to disrupted encoding or retrieval. Studies of functional connectivity between the hippocampus/MTL and default network during naturalistic input have emphasized the interaction between these structures in service of memory encoding and retrieval in the healthy brain (van Kesteren et al., 2010; Chen et al., 2016; Bonasia et al., 2018; Aly et al., 2018), and hippocampal responses at the boundaries between events are theorized to support consolidation of event information (Ben-Yakov et al., 2013; Baldassano et al., 2017; Ben-Yakov and Henson, 2018). Interestingly, MTL damage does not impact connectivity among default network nodes during resting state, but does alter connectivity between the MTL and default network areas (Hayes et al., 2012); in fact, it has been proposed that abnormal hippocampal interactions with other brain regions are the cause of behavioral deficits in amnesia, as opposed to hippocampal damage per se (Argyropoulos et al., 2019). In an experiment closely related to the current study, Oedekoven et al. (2019) scanned a patient with anterograde amnesia resulting from thalamic stroke as they viewed video clips and during later cued retrieval. While no univariate activity differences were observed between the patient and controls during video viewing and retrieval, functional connectivity between bilateral PMC and left hippocampus was reduced in the patient brain relative to controls during both video viewing and retrieval. Such

results are consistent with the notion that interactions between the hippocampus and default network regions are important for long-term encoding and retrieval of semantically rich real-world events.

Within the default network regions of D.A.'s brain, activity patterns in PPC and PMC during narrative listening were relatively preserved. In contrast, activity patterns in mPFC were less preserved. PPC and PMC also demonstrated the “unscrambling” effect in the amnesic brain, while mPFC did not. Interestingly, among default network regions, mPFC is known to be strongly coupled with the hippocampus in studies of resting state connectivity (Kahn et al., 2008) and oscillatory synchrony; in particular, hippocampal-PFC interactions are thought to be crucial for learning and remembering events (Eichenbaum, 2017; van Kesteren et al., 2012). Thus, one might take these results to suggest that the missing interactions with hippocampus caused mPFC activity to diverge from the healthy pattern more than PPC or PMC. However, this interpretation should be treated with great caution, as in this experiment design, between-group divergences are difficult to interpret; differences between the amnesic and healthy brain could arise from a number of plausible sources, such as undiagnosed atrophy or the substantial age difference between the patient (63) and the controls (18–31). Indeed, Campbell et al. (2015) showed that, while brain responses of younger adults were significantly similar to those of older adults during movie viewing in virtually the entire cortex, there were also changes in movie-driven brain responses with age, specifically that ISC was lower among older subjects, i.e., there was increased individual variability. Thus, it is important that our main conclusions are based on similarities between patient and controls, not dissimilarities: the patient's brain activity resembles that of controls during story listening, and is disrupted in the same manner by scrambling paragraphs, showing that at least some portion of long-timescale context sensitivity remains in default network brain activity even in the absence of a functioning hippocampus.

We argue that the default network supports the processing of unfolding narrative information. How does this proposal account for deficits observed in amnesia in non-mnemonic narrative tasks? For example, prior neuropsychological studies have found deficits in high-level narrative coherence in amnesia (e.g., Race et al., 2015a, b), and patient HM is documented as having less globally coherent narratives compared to controls (Mackay, Burke and Stewart, 1998). Our current results show that the long-timescale context sensitivity of default network areas comes at least partly from intrinsic processes, but our observations leave open the (likely) possibility that there is also a contribution from hippocampally-dependent processes. Thus, the deficits in high-level narrative coherence in amnesia could arise from the loss of the hippocampally-dependent component. One possibility is that gist information is supported by default network intrinsic processes, while details are supported by the hippocampus (e.g., Verfaellie et al., 2014). This is not incompatible with our view, which is essentially that the default network carries information about event schemas (Ranganath and Ritchey, 2012). However, this comes with two caveats: 1) the definitions of “gist” and “details” are underspecified, and we are not aware of a field consensus on these definitions; and 2) we would not expect a hippocampal amnesic patient to encode a new “gist” or “event schema” into long-term memory – we would only expect that gist or event schema information could linger longer than details, given that it continues to influence stimulus-locked default network activity for ~30 s during narrative listening. In other words, in healthy brains we expect that the hippocampus is needed to reinstate both schematic context and details in default network areas after a long delay; the hippocampus' role is not necessarily restricted to details.

Our observations may also have implications for the phenomenological experience of amnesics when they listen to stories or watch movies that are multiple minutes long: although they are later unable to report the details, their moment-by-moment comprehension of narratives may be similar to that of healthy individuals in many respects. It has been challenging to concretely assess amnesic patients' experience of minutes-long continuous stimuli like stories. Prose tests tend to be very short,

typically less than 1 min; the Logical Memory Test component of the Wechsler Memory Scale (Wechsler, 1987), a widely-used standard measure of prose memory, is only 65 words long. Amnesic immediate recall performance for short prose passages, while not as catastrophically impaired as after a filled delay, is still poor (Baddeley and Wilson, 2002; Rosenbaum et al., 2008). In verbal discourse about future and past events, amnesics show impairments in both low and high levels of coherence (Kurczek and Duff, 2011; Race et al., 2015a). One challenge in conducting such behavioral tests is that interrupting story-listening to ask questions changes the context and necessarily creates a discontinuity; in other words, testing recall can introduce a discontinuity which hinders recall (Jang and Huber, 2008). Thus, while suggestive, extant behavioral studies do not show that amnesics can follow a narrative multiple minutes long. Our finding that a 63-year-old hippocampal amnesic's brain activity patterns significantly resemble those of young (18–33) healthy controls, moment-by-moment over the course of a 7 min narrative, suggests that recall tests may have underestimated the ability of hippocampal amnesics to integrate naturalistic information over time.

In this paper we present evidence that the purported ability of default network cortical areas to integrate information across long timescales, on the order of 30 s or more, does not depend solely on interactions with the hippocampus. We scanned an amnesic patient with bilateral hippocampal damage as he listened to intact and paragraph-scrambled auditory narratives. Within the default network (PPC and PMC, but not MPFC), the amnesic's moment-by-moment brain activity patterns were significantly similar to that of a healthy control cohort; in the same brain areas, responses were affected by the story scrambling, indicating that they integrated information across paragraphs. The observations in this case study support the idea that default network cortical areas have an intrinsic ability to carry slowly-changing information during semantically rich natural input.

Author contributions

J.C., C.J.H., M.D.B., K.A.N., and U.H. designed the experiment and analyses. M.D.B., J.C., C.J.H., and D.C. collected the data. X.Z., J.C., and D.C. analyzed the data. J.C., X.Z., C.J.H., K.A.N., M.D.B., and U.H. wrote the manuscript.

Acknowledgements

We thank Lok-Kin Yeung and Rachel Newsome for assistance with data collection; we thank Buddhika Bellana, Hongmi Lee, and Lisa Musz for their comments on the manuscript. J.C. was supported by the Sloan Research Fellowship. C.J.H. was supported by the Natural Sciences and Engineering Research Council of Canada (RGPIN-2014-04465) and the Sloan Research Fellowship. M.B. was supported by the Natural Sciences and Engineering Research Council of Canada (RGPIN-2014-05959) and a James S. McDonnell Foundation Scholar Award. K.A.N. and U.H. were supported by the National Institute of Mental Health award R01MH112357.

Appendix A. Supplementary data

Supplementary data to this article can be found online at <https://doi.org/10.1016/j.neuroimage.2020.116658>.

References

- Baxter, M.G., Murray, E.A., 2001. Opposite relationship of hippocampal and rhinal cortex damage to delayed nonmatching-to-sample deficits in monkeys. *Hippocampus* 11, 61–71. [https://doi.org/10.1002/1098-1063\(2001\)11:1<61::AID-HIPO1021>3.0.CO;2-Z](https://doi.org/10.1002/1098-1063(2001)11:1<61::AID-HIPO1021>3.0.CO;2-Z).
- Aly, M., Chen, J., Turk-Browne, N.B., Hasson, U., 2018. Learning naturalistic temporal structure in the posterior medial network. *J. Cognit. Neurosci.* 30, 1345–1365. https://doi.org/10.1162/jocn_a_01308.
- Argyropoulos, G.P., Loane, C., Roca-Fernandez, A., Lage-Martinez, C., Gurau, O., Irani, S.R., Butler, C.R., 2019. Network-wide abnormalities explain memory

- variability in hippocampal amnesia. *eLife* 8, e46156. <https://doi.org/10.7554/eLife.46156>.
- Baddeley, A., Wilson, B.A., 2002. Prose recall and amnesia: implications for the structure of working memory. *Neuropsychologia* 40, 1737–1743. [https://doi.org/10.1016/S0028-3932\(01\)00146-4](https://doi.org/10.1016/S0028-3932(01)00146-4).
- Baldassano, C., Chen, J., Zadbood, A., Pillow, J.W., Hasson, U., Norman, K.A., 2017. Discovering event structure in continuous narrative perception and memory. *Neuron* 95, 709–721. <https://doi.org/10.1016/j.neuron.2017.06.041> e5.
- Baldassano, C., Hasson, U., Norman, K.A., 2018. Representation of real-world event schemas during narrative perception. *J. Neurosci.* 38, 9689–9699. <https://doi.org/10.1523/JNEUROSCI.0251-18.2018>.
- Ben-Yakov, A., Henson, R.N., 2018. The hippocampal film editor: sensitivity and specificity to event boundaries in continuous experience. *J. Neurosci.* 38, 10057–10068. <https://doi.org/10.1523/JNEUROSCI.0524-18.2018>.
- Ben-Yakov, A., Eshel, N., Dudai, Y., 2013. Hippocampal immediate poststimulus activity in the encoding of consecutive naturalistic episodes. *J. Exp. Psychol. Gen.* 142, 1255–1263. <https://doi.org/10.1037/a0033558>.
- Benjamini, Y., Hochberg, Y., 1995. Controlling the False Discovery rate: a practical and powerful approach to multiple testing. *J. R. Stat. Soc. Ser. B Methodol.* 57, 289–300. <https://doi.org/10.1111/j.2517-6161.1995.tb02031.x>.
- Bonasia, K., Sekeres, M.J., Gilboa, A., Grady, C.L., Winocur, G., Moscovitch, M., 2018. Prior knowledge modulates the neural substrates of encoding and retrieving naturalistic events at short and long delays. *Neurobiol. Learn. Mem.*, MCCS 2018: Time and Memory 153, 26–39. <https://doi.org/10.1016/j.nlm.2018.02.017>.
- Campbell, K.L., Shafto, M.A., Wright, P., Tsvetanov, K.A., Geerligs, L., Cusack, R., Tyler, L.K., Brayne, C., Bullmore, E., Calder, A., Cusack, R., Dalgleish, T., Duncan, J., Henson, R., Matthews, F., Marslen-Wilson, W., Rowe, J., Shafto, M., Campbell, K., Cheung, T., Davis, S., Geerligs, L., Kievit, R., McCarrey, A., Price, D., Taylor, J., Tsvetanov, K., Williams, N., Bates, L., Emery, T., Erzinçoglu, S., Gadie, A., Gerbase, S., Georgieva, S., Hanley, C., Parkin, B., Troy, D., Allen, J., Amery, G., Amunts, L., Barcroft, A., Castle, A., Dias, C., Dowrick, J., Fair, M., Fisher, H., Goulding, A., Grewal, A., Hale, G., Hilton, A., Johnson, F., Johnston, P., Kavanagh-Williamson, T., Kwasniewska, M., McMinn, A., Norman, K., Penrose, J., Roby, F., Rowland, D., Sargeant, J., Squire, M., Stevens, B., Stoddart, A., Stone, C., Thompson, T., Yazlik, O., Dixon, M., Barnes, D., Hillman, J., Mitchell, J., Villis, L., Tyler, L.K., 2015. Idiosyncratic responding during movie-watching predicted by age differences in attentional control. *Neurobiol. Aging* 36, 3045–3055. <https://doi.org/10.1016/j.neurobiolaging.2015.07.028>.
- Chaudhuri, R., Knoblauch, K., Gariel, M.A., Kennedy, H., Wang, X.J., 2015. A Large-Scale Circuit Mechanism for Hierarchical Dynamical Processing in the Primate Cortex. *Neuron* 88, 419–431. <https://doi.org/10.1016/j.neuron.2015.09.008>.
- Chen, J., Honey, C.J., Simony, E., Arcaro, M.J., Norman, K.A., Hasson, U., 2016. Accessing real-life episodic information from minutes versus hours earlier modulates hippocampal and high-order cortical dynamics. *Cerebr. Cortex* 26, 3428–3441. <https://doi.org/10.1093/cercor/bhv155>.
- Chen, J., Leong, Y.C., Honey, C.J., Yong, C.H., Norman, K.A., Hasson, U., 2017. Shared memories reveal shared structure in neural activity across individuals. *Nat. Neurosci.* 20, 115–125. <https://doi.org/10.1038/nn.4450>.
- Crawford, J.R., Howell, D.C., 1998. Comparing an Individual's Test Score Against Norms Derived from Small Samples. *Clin. Neuropsychol.* 12, 482–486. <https://doi.org/10.1076/clin.12.4.482.7241>.
- Eichenbaum, H., 2017. Prefrontal-hippocampal interactions in episodic memory. *Nat. Rev. Neurosci.* 18, 547–558. <https://doi.org/10.1038/nrn.2017.74>.
- Frings, L., Schulze-Bonhage, A., Spreer, J., Wagner, K., 2009. Remote effects of hippocampal damage on default network connectivity in the human brain. *J. Neurol.* 256, 2021–2029. <https://doi.org/10.1007/s00415-009-5233-0>.
- Hasson, U., Yang, E., Vallines, I., Heeger, D.J., Rubin, N., 2008. A hierarchy of temporal receptive windows in human cortex. *J. Neurosci.* 28, 2539–2550.
- Hasson, U., Chen, J., Honey, C.J., 2015. Hierarchical process memory: memory as an integral component of information processing. *Trends Cognit. Sci.* 19, 304–313.
- Hayes, S.M., Salat, D.H., Verfaellie, M., 2012. Default network connectivity in medial temporal lobe amnesia. *J. Neurosci.* 32, 14622–14629a. <https://doi.org/10.1523/JNEUROSCI.0700-12.2012>.
- Honey, C.J., Thesen, T., Donner, T.H., Silbert, L.J., Carlson, C.E., Devinsky, O., Doyle, W.K., Rubin, N., Heeger, D.J., Hasson, U., 2012. Slow cortical dynamics and the accumulation of information over long timescales. *Neuron* 76, 423–434.
- Jang, Y., Huber, D.E., 2008. Context retrieval and context change in free recall: recalling from long-term memory drives list isolation. *J. Exp. Psychol. Learn. Mem. Cogn.* 34, 112–127. <https://doi.org/10.1037/0278-7393.34.1.112>.
- Kahn, I., Andrews-Hanna, J.R., Vincent, J.L., Snyder, A.Z., Buckner, R.L., 2008. Distinct cortical anatomy linked to subregions of the medial temporal lobe revealed by intrinsic functional connectivity. *J. Neurophysiol.* 100, 129–139. <https://doi.org/10.1152/jn.00077.2008>.
- Keven, N., Kurczek, J., Rosenbaum, R.S., Craver, C.F., 2018. Narrative construction is intact in episodic amnesia. *Neuropsychologia* 110, 104–112. <https://doi.org/10.1016/j.neuropsychologia.2017.07.028>. Special Issue: Autobiographical Memory.
- Kopelman, M.D., 1987. Two types of confabulation. *J. Neurol. Neurosurg. Psychiatry* 50, 1482–1487. <https://doi.org/10.1136/jnnp.50.11.1482>.
- Kriegeskorte, N., Mur, M., Bandettini, P., 2008. Representational similarity analysis – connecting the branches of systems neuroscience. *Front. Syst. Neurosci.* <https://doi.org/10.3389/fnro.2008.004.2008>.
- Kurczek, J., Duff, M.C., 2011. Cohesion, coherence, and declarative memory: discourse patterns in individuals with hippocampal amnesia. *Aphasiology* 25, 700–712. <https://doi.org/10.1080/02687038.2010.537345>.
- Lerner, Y., Honey, C.J., Katkov, M., Hasson, U., 2014. Temporal scaling of neural responses to compressed and dilated natural speech. *J. Neurophysiol.* 111, 2433–2444. <https://doi.org/10.1152/jn.00497.2013>.
- Lerner, Y., Honey, C.J., Silbert, L.J., Hasson, U., 2011. Topographic mapping of a hierarchy of temporal receptive windows using a narrated story. *J. Neurosci.* 31, 2906–2915. <https://doi.org/10.1523/JNEUROSCI.3684-10.2011>.
- MacKay, D.G., Burke, D.M., Stewart, R., 1998. H.M.'s Language Production Deficits: Implications for Relations between Memory, Semantic Binding, and the Hippocampal System. *Journal of Memory and Language* 38, 28–69. <https://doi.org/10.1006/jmla.1997.2544>.
- McCormick, C., Quraan, M., Cohn, M., Valiante, T.A., McAndrews, M.P., 2013. Default mode network connectivity indicates episodic memory capacity in mesial temporal lobe epilepsy. *Epilepsia* 54, 809–818. <https://doi.org/10.1111/epi.12098>.
- Milner, B., 1966. Amnesia following operation on the temporal lobes. In: *Butterworths, C.W.M. Whitty, Zangwill, O.L. (Eds.), Amnesia, pp. 109–133. London.*
- Milner, B., 2005. The medial temporal-lobe amnesic syndrome. *Psychiatr. Clin.* 28, 599–611. <https://doi.org/10.1016/j.jpsc.2005.06.002>.
- Nastase, S.A., Gazzola, V., Hasson, U., Keysers, C., 2019. Measuring shared responses across subjects using intersubject correlation. *bioRxiv*. <https://doi.org/10.1101/600114>, 600114.
- Oedekoven, C.S.H., Keidel, J.L., Berens, S.C., Bird, C.M., 2017. Reinstatement of memory representations for lifelike events over the course of a week. *Sci. Rep.* 7, 14305. <https://doi.org/10.1038/s41598-017-13938-4>.
- Oedekoven, C.S.H., Keidel, J.L., Anderson, S., Nisbet, A., Bird, C.M., 2019. Effects of amnesia on processing in the hippocampus and default mode network during a naturalistic memory task: a case study. *Neuropsychologia*. <https://doi.org/10.1016/j.neuropsychologia.2019.05.022>.
- Race, E., Keane, M.M., Verfaellie, M., 2015a. Sharing mental simulations and stories: hippocampal contributions to discourse integration. *Cortex* 63, 271–281. <https://doi.org/10.1016/j.cortex.2014.09.004>.
- Race, E., Palombo, D.J., Cadden, M., Burke, K., Verfaellie, M., 2015b. Memory integration in amnesia: prior knowledge supports verbal short-term memory. *Neuropsychologia* 70, 272–280. <https://doi.org/10.1016/j.neuropsychologia.2015.02.004>.
- Rosenbaum, R.S., Moscovitch, M., Poster, J.K., Schnyer, D.M., Gao, F., Kovacevic, N., Verfaellie, M., Black, S.E., Levine, B., 2008. Patterns of autobiographical memory loss in medial-temporal lobe amnesic patients. *J. Cognit. Neurosci.* 20, 1490–1506. <https://doi.org/10.1162/jocn.2008.20105>.
- Ranganath, C., Ritchey, M., 2012. Two cortical systems for memory-guided behaviour. *Nat. Rev. Neurosci.* 13, 713–726. <https://doi.org/10.1038/nrn3338>.
- Rosenbaum, R.S., Gilboa, A., Levine, B., Winocur, G., Moscovitch, M., 2009. Amnesia as an impairment of detail generation and binding: evidence from personal, fictional, and semantic narratives in K.C. *Neuropsychologia*. *Episodic Mem. Brain* 47, 2181–2187. <https://doi.org/10.1016/j.neuropsychologia.2008.11.028>.
- Schaefer, A., Kong, R., Gordon, E.M., Laumann, T.O., Zuo, X.-N., Holmes, A.J., Eickhoff, S.B., Yeo, B.T.T., 2018. Local-global parcellation of the human cerebral cortex from intrinsic functional connectivity MRI. *Cerebr. Cortex* 28, 3095–3114. <https://doi.org/10.1093/cercor/bhx179>.
- Simony, E., Honey, C.J., Chen, J., Lositsky, O., Yeshurun, Y., Wiesel, A., Hasson, U., 2016. Dynamic reconfiguration of the default mode network during narrative comprehension. *Nat. Commun.* 7. <https://doi.org/10.1038/ncomms12141>.
- Squire, L.R., Zola-Morgan, M., 1991. The cognitive neuroscience of human memory since H.M. *Annu. Rev. Neurosci.* 34, 259–288. <https://doi.org/10.1146/annurev-neuro-061010-113720>.
- Stephens, G.J., Honey, C.J., Hasson, U., 2013. A place for time: the spatiotemporal structure of neural dynamics during natural audition. *J. Neurophysiol.* 110, 2019–2026. <https://doi.org/10.1152/jn.00268.2013>.
- van Kesteren, M.T.R., Fernandez, G., Norris, D.G., Hermans, E.J., 2010. Persistent schema-dependent hippocampal-neocortical connectivity during memory encoding and postencoding rest in humans. *Proc. Natl. Acad. Sci. Unit. States Am.* 107, 7550–7555. <https://doi.org/10.1073/pnas.0914892107>.
- van Kesteren, M.T.R., Ruiters, D.J., Fernández, G., Henson, R.N., 2012. How schema and novelty augment memory formation. *Trends Neurosci.* 35, 211–219. <https://doi.org/10.1016/j.tins.2012.02.001>.
- Verfaellie, M., Bousquet, K., Keane, M.M., 2014. Medial temporal and neocortical contributions to remote memory for semantic narratives: Evidence from amnesia. *Neuropsychologia* 61, 105–112. <https://doi.org/10.1016/j.neuropsychologia.2014.06.018>.
- Wechsler, D., 1987. *WMS-R: Wechsler Memory Scale-Revised: Manual.* Harcourt Brace Jovanovich, San Antonio.
- Yeo, B.T.T., Krienen, F.M., Sepulcre, J., Sabuncu, M.R., Lashkari, D., Hollinshead, M., Roffman, J.L., Smoller, J.W., Zöllei, L., Polimeni, J.R., Fischl, B., Liu, H., Buckner, R.L., 2011. The organization of the human cerebral cortex estimated by intrinsic functional connectivity. *J. Neurophysiol.* 106, 1125–1165. <https://doi.org/10.1152/jn.00338.2011>.